Final Report

Project Title: Chemical Optimization of the Caged Garcinia Xanthone Pharmacophore

By Dr. Oraphin Chantarasriwong

1 December 2016

Contact No. TRG5780085

Final Report

Project Title: Chemical Optimization of the Caged Garcinia Xanthone Pharmacophore

Dr. Oraphin Chantarasriwong
Department of Chemistry, King Mongkut's University of Technology Thonburi

This project granted by the Thailand Research Fund and King Mongkut's University of Technology Thonburi

Abstract

Project Code : TRG5780085

Project Title : Chemical Optimization of the Caged Garcinia Xanthone Pharmacophore

Investigator : Dr. Oraphin Chantarasriwong
(King Mongkut's University of Technology Thonburi)

E-mail Address : oraphin.cha@kmutt.ac.th

Project Period : 2 June 2014 - 1 December 2016

This project aims to synthesize cluvenone derivatives for the antimalarial activity against *Plasmodium falciparum*. The results showed that **CR135** and **CR142** show highly effective antimalarial inhibitors with the EC_{50} values of 7.9 and 11.1 nM, respectively, suggesting that attaching a triphenylphosphonium group at the A ring of the cluvenone could improve activity.

In addition, this project aims to develop a new method for *N*-*tert*-butyloxycarbonylation of amines using brominating agents as a catalyst. *N*-bromosuccinimide (NBS) and hexabromoacetone ($Br_3CCOCBr_3$) are new and efficient catalysts for the chemoselective *N*-*tert*-butyloxycarbonylation of aliphatic and aromatic amines. This method is novel, simple and effective for the preparation of *N*-Boc protected products in good to excellent yields with short reaction times at room temperature.

Keywords : Caged Garcinia xanthone; Gambogic acid; Cluvenone; Antimalarial activities; *N*-*tert*-Butyloxycarbonylation

บทคัดย่อ

รหัสโครงการ : TRG5780085

ชื่อโครงการ : การหาโครงสร้างทางเคมีที่ดีที่สุดต่อการออกฤทธิ์ทางเภสัชวิทยาของสารกลุ่ม Caged Garcinia Xanthone

ชื่อนักวิจัยและสถาบัน : ดร. อรพิน จันทรศรีวงศ์ ภาควิชาเคมี คณะวิทยาศาสตร์ มหาวิทยาลัยเทคโนโลยีพระจอมเกล้าธนบุรี

E-mail Address : oraphin.cha@kmutt.ac.th

ระยะเวลาดำเนินโครงการ : 2 มิถุนายน 2557 – 1 ธันวาคม 2559

งานวิจัยฉบับนี้มุ่งเน้นเพื่อที่จะสังเคราะห์อนุพันธ์ของ cluvenone สำหรับฤทธิ์การต้านมาลาเรีย *Plasmodium falciparum* จากผลการทดลองพบว่า **CR135** and **CR142** แสดงฤทธิ์การต้านมาลาเรียที่ดีด้วยค่า EC_{50} เท่ากับ 7.9 และ 11.1 นาโนโมลาร์ ตามลำดับ ซึ่งชี้ให้เห็นว่าการเชื่อมต่อหมู่ triphenylphosphonium ที่วง A ของ cluvenone สามารถปรับปรุงแสดงฤทธิ์การต้านมาลาเรีย

นอกจากนี้ในงานวิจัยนี้ยังมุ่งเน้นเพื่อที่จะพัฒนาวิธีการใหม่สำหรับ *N-tert*-butyloxycarbonylation ของเอมีน โดยใช้โบรมิเนทิงเอเจนต์เป็นตัวเร่งปฏิกิริยา *N*-bromosuccinimide (NBS) และ hexabromoacetone ($Br_3CCOCBr_3$) คือตัวเร่งปฏิกิริยาใหม่และมีประสิทธิภาพสำหรับ *N-tert*-butyloxycarbonylation ของแอลิฟาติกเอมีนและแอโรมาติกเอมีนที่มีความเลือกจำเพาะทางเคมี วิธีการนี้เป็นวิธีการใหม่ ง่าย และมีประสิทธิภาพสำหรับการเตรียมผลิตภัณฑ์ในปริมาณดีถึงสูง ด้วยเวลาในการทำปฏิกิริยาน้อยที่อุณหภูมิห้อง

คำหลัก: Caged Garcinia xanthone; Gambogic acid; Cluvenone; ฤทธิ์การต้านมาลาเรีย; *N-tert*-Butyloxycarbonylation

1. Executive summary

This research was divided into two parts:

Part I: Chemical optimization of the caged Garcinia xanthone pharmacophore

This part is a reprint of the material as it appears in Antimicrobial Agents and Chemotherapy **2016**. Hangjun Ke, Joanne M. Morrisey, Shiwei Qu, Oraphin Chantarasriwong, Michael W. Mather, Emmanuel A. Theodorakis and Akhil B. Vaidya. Caged Garcinia xanthones: a novel chemical scaffold with potent antimalarial activity. *Antimicrobial Agents and Chemotherapy*, **2016**. (Accepted manuscript posted online 31 October 2016, doi: 10.1128/AAC.01220-16)

The *Garcinia* plants have yielded an intriguing family of caged xanthone-derived natural products that have a documented value in traditional eastern medicine.[1] Studies from different laboratories have shown that selected members of the caged *Garcinia* xanthones possess several essential characteristics that highlight clearly their enormous potential in drug discovery. However, the full biological evaluation of caged *Garcinia* xanthones could not be accomplished because often they are complex and difficult to synthesize, found in low quantities, and produced by undomesticated and rare plants. As such, it represents the most synthetically challenging for identification and optimization of caged *Garcinia* xanthone pharmacophore.

Malaria remains a leading infectious disease in the tropical and subtropical regions of the world. In the past 15 years, the morbidity and mortality of malaria has decreased dramatically due to the wide use of artemisinin-combined chemotherapy, indoor residual spraying, the distribution of insecticide-treated bed nets, and other malaria prevention and research efforts.[2-4] However, malaria parasites have evolved mechanisms to adapt to various hosts and environmental surroundings. The recent appearance and spread of artemisinin tolerance underscores the need for continued urgent efforts to develop new antimalarial reagents.[5-7] Since malaria parasites require mitochondrial functions for survival, we speculated that gamboic acid and their derivatives might exhibit antimalarial activity. The structure-activity relationship studies of of gambogic acid and synthetic cluvenone analogues against the human malaria parasite *Plasmodium falciparum* showed that cluvenone derivatives **CR135** and **CR142** presented highly effective antimalarial inhibitors with the EC_{50} values of 7.9 and 11.1 nM, respectively, suggesting that attaching a triphenylphosphonium

group at the A ring of the cluvenone could improve activity. These studies produce new antimalarial drug candidates and have a significant impact to public health.

Part II: Facile methodology for chemoselective *N*-*tert*-butyloxycarbonylation of amines using brominating agent as a catalyst

This part is a reprint of the material as it appears in Tetrahedron letters **2016**. Oraphin Chantarasriwong,* Banphot Jiangchareon, Christian Kurnia Putra, Winai Suwankrua, Warinthorn Chavasiri "NBS and Br_3 $CCOCBr_3$ as highly efficient catalysts for the chemoselective *N*-tert-butyloxycarbonylation of amines" *Tetrahedron Letters*, **2016**, *57*, 4807–4811.

The protection of amino groups plays a significant role in the multi-step synthesis of peptides and nitrogen-containing pharmaceuticals.[8] The most frequently employed amine protection methods involve the formation of an *N*-*tert*-butoxycarbonyl (*N*-Boc) group due to its stability toward catalytic hydrogenation, base and nucleophilic attack, as well as the ease of removal under mild acidic conditions.[9] The *N*-Boc group is frequently introduced by the treatment of amines with di-*tert*-butyl dicarbonate [$(Boc)_2O$] because of its low price, commercial availability, stability and efficiency.[2] Organic and inorganic bases, including DMAP,[10] NaOH,[11] NH_2OH,[12] NaHMDS[13] and K_2CO_3,[14] have been used as reagents or catalysts, however these methods present certain disadvantages including long reaction times, use of an excess of reagents, unsatisfactory yields, and the formation of isocyanates, ureas, or *N*,*N*-di-Boc derivatives as by-products.[15] Alternatively, methods involving Lewis/ Brønsted acid,[16-33] heterogeneous catalysts,[34-46] and acidic ionic liquids[47-53] have also been used for the *N*-*tert*-butoxycarbonylation of amines. Other procedures have also been reported, including the use of β-cyclodextrin,[54] catalyst-free reactions in water,[55] ethanol[56] and polyethylene glycols[57, 58] as well as solvent-free conditions with and without microwave irradiation.[59-61] Although these methodologies provide a marked improvement over past methods, some still possess drawbacks such as moisture-sensitive reagents, prolonged reaction times, time consuming work-up processes, harsh conditions and tedious steps needed for the preparation of reagents/catalysts. As a result, the development of new, facile and effective methods for the *N*-*tert*-butyloxycarbonylation of amines still represents a desirable goal. To the best of our knowledge, few reports exist concerning the use of $Br_3CCOCBr_3$ for organic reactions[61, 62] and there are no reports on the utilization of NBS and $Br_3CCOCBr_3$ as

catalysts for *N-tert*-butyloxycarbonylation of amines. Therefore, we describe herein the use of NBS and $Br_3CCOCBr_3$ as catalysts in the *N-tert*-butyloxycarbonylation of amines under mild reaction conditions. The results showed that NBS and $Br_3CCOCBr_3$ were new and efficient catalysts for the chemoselective *N*-tert-butyloxycarbonylation of aliphatic and aromatic amines. This method is novel, simple and effective for the preparation of N-Boc protected products in good to excellent yields (62-100%) with short reaction times at room temperature. Highly chemoselective reactions were also performed using amines containing two different types of amino groups, only primary amino groups were protected to give the corresponding mono *N*-Boc products in excellent yields. In addition, in the case of amino acid esters, L-alanine ethyl ester and L-phenylalanine methyl ester converted to the corresponding *N*-Boc products in good to excellent yields (82-98%) without racemization

2. Objective

PART I: Chemical optimization of the caged Garcinia xanthone pharmacophore

2.1 Synthesize and optimize the structure of cluvenone derivatives.

2.2 Screen the synthetic cluvenone derivatives for antimalarial activity.

PART II: Facile methodology for chemoselective *N*-tert-butyloxycarbonylation of amines using brominating agent as a catalyst

2.3 Develop the method for chemoselective *N*-tert-butyloxycarbonylation of amines using brominating agent as a catalyst

3. Research methodology

3.1 Review the literatures with regard to chemistry and biology of caged Garcinia xanthones and *N*-tert-butyloxycarbonylation of amines

PART I: Chemical optimization of the caged Garcinia xanthone pharmacophore

3.2 Isolate gambogic acid from gamboge

Dried powder of gamboge (19.0 g) from the *G. hurburyi* tree was extracted with MeOH (80 mL) at room temperature for a day. The mixture was filtered and the residue was re-extracted two more times with MeOH (80 mL). The combined filtrate

was concentrated under reduced pressure to give crude extract as a yellow powder (13.0 g, 68%). The crude extract (13.0 g) was dissolved in pyridine (13 mL), and then warm water (5 mL) was added to the stirred solution. The reaction mixture was cooled to room temperature and some precipitate was observed. Hexane (10 mL) was added to the mixture and the mixture was filtered. The solid was collected and washed with hexane and dried to yield pyridine salt of gambogic acid as a yellow solid (1.8 g, 14%).

To a solution of the pyridine salt of GA (1.26 g, 1.77 mmol) in ether (20 mL) was added aqueous HCl (1N, 12.6 mL). After 1 h of continued stirring at room temperature, the ether solution was washed with water (3 x 3 mL), dried over $MgSO_4$, and concentrated by rotary evaporation to give GA as a yellow solid (1.10 mg, 99%).

3.3 Synthesize Cluvenone (CLV).

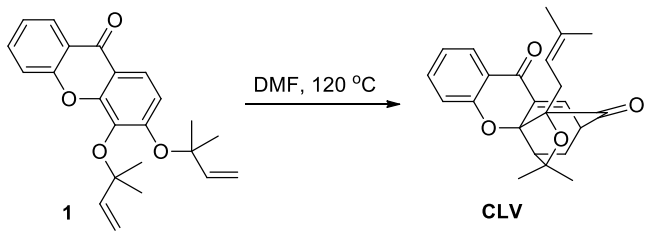

A solution of compound **1** (350 mg, 0.96 mmol) in DMF (6 mL) was heated at 120 ˚C for 1.5 hours. The onset of a yellow color indicated the formation of cluvenone. The reaction mixture was then cooled to room temperature and the solvent was removed by rotary evaporation. The crude material was then purified by column chromatography (silica, 20-30% Et2O-hexane) to yield cluvenone (285 mg, 81%).

3.4 Synthesize MAD28

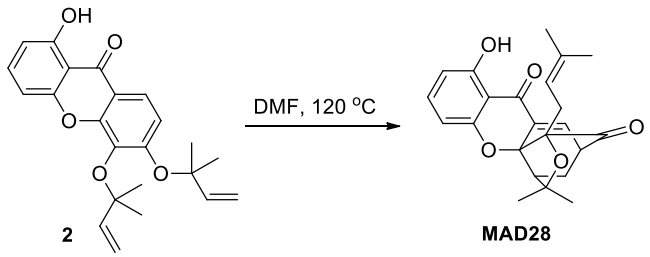

A solution of **2** (106.5 mg, 0.280 mmol) in anhydrous DMF (3 mL) was stirred at 120 °C for 2 hours. The mixture was then cooled to room temperature and the solvent was removed under reduced pressure. The residue was then purified by column chromatography (silica gel, EtOAc/hexane = 1:10) to afford MAD28 (101.2 mg, 95%) as a yellow solid.

3.5 Synthesize CR135

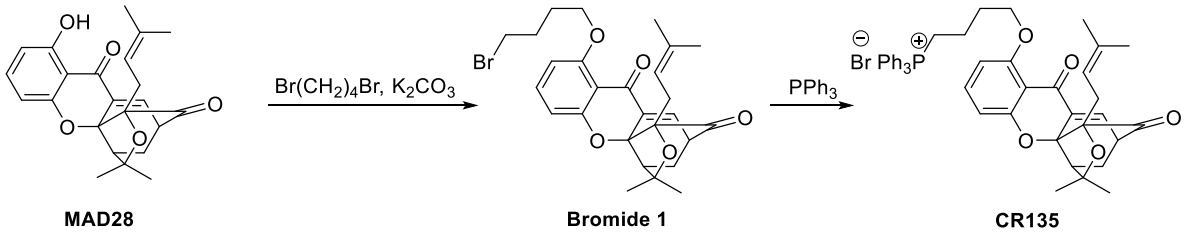

To a solution of MAD28 (50 mg, 0.13 mmol) in DMF (1 mL), potassium carbonate (36 mg, 0.26 mmol) and 1, 4-dibromobutane (140 mg, 0.65 mmol) were added. The mixture was left stirring at 80°C during 16 h. Upon completion, the reaction mixture was quenched with water (3 mL) and extracted with diethyl ether (2 × 10 mL). The combined organic layers were washed with brine, dried over $MgSO_4$, filtered, and concentrated in vacuum. Purification by flash column chromatography (silica, 30% EtOAc-hexane) gave bromide 1 (45.6 mg, 88.4 μmol, 68% yield).

To a solution of Bromide 1 (35 mg, 67.9 μmol) in acetonitrile (1 mL), triphenylphosphine (89 mg, 0.34 mmol) was added. The mixture was stirred under a microwave irradiation for 2 h at 150°C. Upon completion, the reaction mixture was cooled to room temperature and the excess acetonitrile was removed by rotary evaporation. The crude was dissolved in DCM (1 mL) and hexane (10 mL) was added. The solid was filtered and washed with hexane to yield CR135 (44.9 mg, 57.7 μmol, 85% yield).

3.6 Synthesize CR142

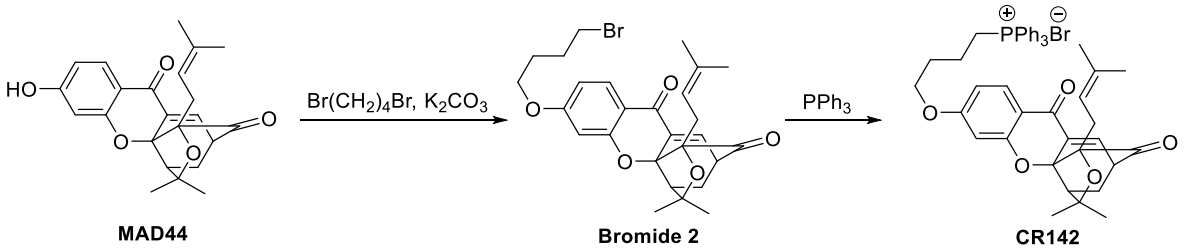

To a solution of MAD44 (0.1g, 0.26 mmol) in DMF (2 mL), potassium carbonate (72 mg, 0.52 mmol) and 1, 4-dibromobutane (0.28 g, 1.31 mmol) were added. The mixture was left stirring at room temperature during 8 h. Upon completion, the reaction mixture was quenched with water (10 mL) and extracted with diethyl ether (2 × 20 mL). The combined organic layers were washed with brine, dried over $MgSO_4$,

filtered, and concentrated in vacuo. Purification by flash column chromatography (silica, 30% EtOAc-hexane) gave bromide 2 (0.11 g, 0.22 mmol, 85% yield).

To a solution of Bromide 2 (0.1 g, 0.19 mmol) in acetonitrile (5 mL), triphenylphosphine (0.25 g, 0.97 mmol) was added. The mixture was stirred under a microwave irradiation for 2 h at 150°C. Upon completion, the reaction mixture was cooled to room temperature and the excess acetonitrile was removed by rotary evaporation. The crude was dissolved in DCM (3 mL) and hexane (30 mL) was added. The solid was filtered and washed with hexane to yield CR142 (0.15 g, 0.18 mmol, 98% yield).

3.7 Study the antimalarial activity of gambogic acid, cluvenone and cluvenone derivatives.

PART II: Facile methodology for chemoselective *N*-tert-butyloxycarbonylation of amines using brominating agent as a catalyst

3.8 Optimize the reaction condition for *N-tert*-butoxycarbonylation of amines by studying the effect of catalyst type and amount.

General procedure for *N-tert*-butoxycarbonylation of amines: To a stirred solution of a selected amine (1 mmol, 1 equiv.) and $(Boc)_2O$ (1 mmol, 1 equiv.) in CH_2Cl_2 (0.2 mL) was added catalyst (0.1 mmol, 0.1 equiv.) at room temperature. The mixture was stirred for the indicated time and the progress was monitored using TLC. After completion, the solvent was removed under reduced pressure and the product was purified by flash column chromatography (SiO_2, hexane/ethyl acetate 15:1 to 10:1).

3.9 Study the scope and limitation of the optimized reaction condition by varying amine types.

3.10 Study the chemoselectivity of *N-tert*-butoxycarbonylation of amines.

3.11 Study the mechanism of *N-tert*-butoxycarbonylation of amines using IR analysis.

3.12 Characterize the identity of products using ^{1}H NMR, ^{13}C NMR and MS spectrometer.

3.13 Compile the results and discussion.

3.14 Draft the manuscript for international paper submission.

4. Results and discussion

PART I: Chemical optimization of the caged Garcinia xanthone pharmacophore

The erythrocytic stage of malaria parasites causes all clinical symptoms associated with malaria and is the target for most antimalarial drugs. *P. falciparum* strains isolated from various geographical regions harbor different sensitivities to antimalarial drugs. Dd2 is a multi-drug resistant clone selected from an Indochina isolate using mefloquine pressure.[63] To test if gambogic acid and related cluvenone analogues (see structure in Figure 1) have activities against drug resistant parasites, we performed growth inhibition assays based on ^{3}H-hypoxanthine incorporation by Dd2 parasites (Figure 2). Artemisinin was included as a control in this assay, which displayed an EC_{50} value of 10.4 nM.[64] As shown in Figure 2, gambogic acid and Cluvenone (CLV) exhibited moderate antimalarial activities with EC_{50} values of 0.27 μM and 0.43 μM, respectively. A similar antimalarial activity was observed with **MAD28**, the C6 hydroxylated cluvenone, which exhibited an EC_{50} of 0.26 μM. However, **MAD44**, the C18 hydroxylated cluvenone, was less effective, with an EC_{50} of 4.0 μM. **CR135** and **CR142** were synthesized from **MAD28** and **MAD44**, respectively, by conjugating a triphenylphosphonium group at C6 of **MAD28** and C18 of **MAD44**.[65]

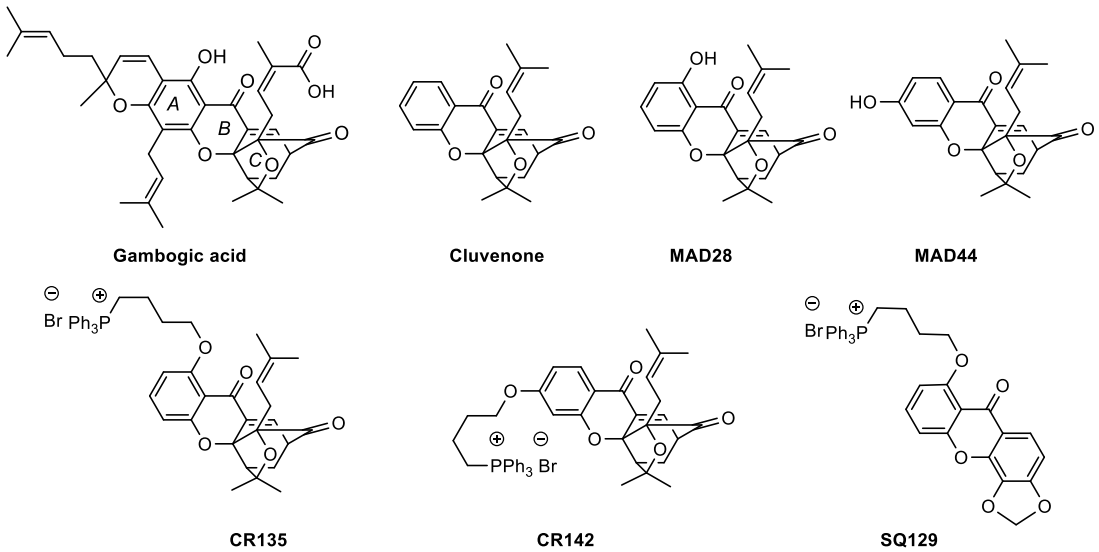

Figure 1. Chemical structures of gambogic acid and cluvenone derivatives

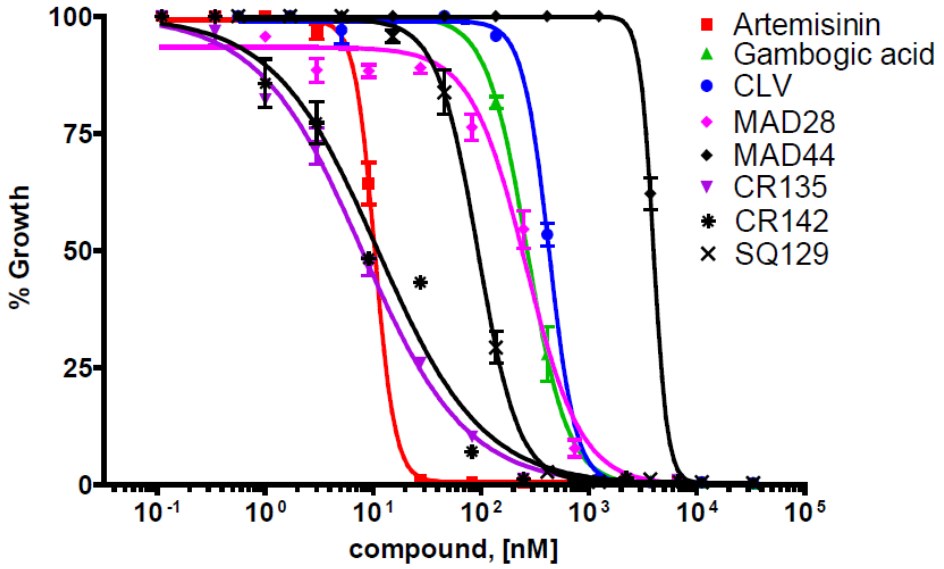

Figure 2. The antimalarial effect of caged Garcinia compounds in *P. falciparum* parasites. The x axis indicates the concentrations of a tested compound, and the y axis indicates the percentage of ^{3}H-hypoxanthine incorporation compared to that in no-drug controls.

Importantly, **CR135** and **CR142** exhibited remarkable antimalarial activities, with EC50s of 7.9 nM and 11.1 nM, respectively. Thus, conjugating the A ring of the caged xanthone structure with a triphenylphosphonium group drastically improves the antimalarial activity. Specifically, adding this group to the C6-hydroxyl group of **MAD28** decreased the EC_{50} by about 30 fold from 262 nM (**MAD28**) to 7.9 nM (**CR135**). The same modification at the C18-hydroxyl group decreased the EC50 about 360 fold from 3972 nM (**MAD44**) to 11.1 nM (**CR142**). To test if a caged xanthone was required for the robust activity of **CR135**, we replaced the caged xanthone structure of **CR135** with a planar xanthone, yielding the compound **SQ129**. The antimalarial activity of **SQ129** (EC50, 114 nM) was much weaker 207 than that of **CR135**, suggesting that a caged xanthone moiety is also needed for optimal antimalarial activity.

PART II: Facile methodology for chemoselective *N*-tert-butyloxycarbonylation of amines using brominating agent as a catalyst

The effect of catalyst type and amount was initially investigated using 4-chloroaniline (**1**, 1 mmol) as a model substrate for the reaction with di-*tert*-butyl dicarbonate ($(Boc)_2O$, 1 mmol) in CH_2Cl_2 (0.2 mL) at room temperature (Table 1).

In the absence of catalyst, the *N*-Boc protected product was isolated in only 35% yield after 24 h (Entry 1). To improve the yield, different catalysts containing bromine atoms were employed. A moderate yield of the desired product was achieved when carrying out the reaction with CBr_4 and $CHBr_3$ (57-65%, Entries 2 and 3). The use of 10 mol% NBS led to an almost quantitative yield of the desired product within 2 h at room temperature (Entry 4). $Br_3CCOCBr_3$ also produced the desired product quantitatively, whereas HBr gave the desired product in 22% yield after 24 h (Entries 6 and 8). With the intention of using the lowest possible amount of catalyst, the amount of NBS and $Br_3CCOCBr_3$ were reduced to 5 mol%, resulting in significant decreases in yield to 43% and 54%, respectively (Entries 5 and 7). These results indicated that 10 mol% of NBS and $Br_3CCOCBr_3$ were optimal for the *N*-*tert*-butyloxycarbonylation of amines with $(Boc)_2O$.

Table 1. Effect of catalyst type and amount on the *N*-*tert*-butyloxycarbonylation of 4-chloroaniline (**1**)

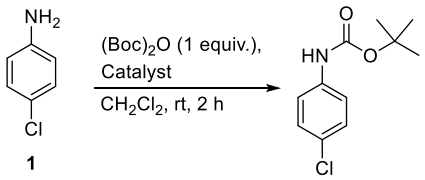

1
1 mmol, 1 equiv.

1a

Entry	Catalyst		Yield[a] (%)
	Type	mol%	
1	None	-	35[b]
2	CBr_4	10	65
3	$CHBr_3$	10	57
4	NBS	10	96
5	NBS	5	43
6	$Br_3CCOCBr_3$	10	quant.
7	$Br_3CCOCBr_3$	5	54
8	HBr	10	22[b]

[a] Isolated yield.
[b] 24 h.

With the optimal reaction conditions established, the limitations and generality of the method were examined by the *N*-*tert*-butyloxycarbonylation of various aliphatic amines (Table 2). The reaction of primary and secondary aliphatic amines with $(Boc)_2O$ in the presence of 10 mol% NBS or $Br_3CCOCBr_3$ proceeded quickly. The *N*-Boc protected products were isolated in good to excellent yields (62-100%, Entries 1-17) within 5 min to 2 h without the formation of by-products such as urea and isocyanate derivatives. The steric hindrance of the amines had effect on the reaction rates or product yields. For example, the sterically hindered *tert*-butyl amine required longer reaction times than *n*-butylamine and *sec*-butylamine to achieve good product yields (Entries 1 and 2 vs. 3). In the case of the chiral amine (*R*)-(+)-1-phenylethylamine, both NBS and $Br_3CCOCBr_3$ gave the optically pure *N*-Boc protected product (as determined by the optical rotation and comparison with literature values)[66] in nearly quantitative yield after 5 min (Entry 8). Ethanolamine, morpholine and dimethylaminoacetal were chemoselectively converted into the corresponding *N*-Boc protected products in near quantitative yields without any *O*-Boc protected products formed (Entries 11-13). Highly chemoselective reactions were also performed using amines containing two different types of amino groups, such as 3-picolylamine and phenylhydrazine, only primary amino groups were protected to give the corresponding mono *N*-Boc products in excellent yields (Entries 14-15). In the case of amino acid esters, L-alanine ethyl ester and L-phenylalanine methyl ester converted to the corresponding *N*-Boc products in good to excellent yields (82-98%, Entries 16 and 17) without racemization as determined by the optical rotation and their specific rotation values are consistent with the reported data.[55, 67] Since primary aliphatic amines are very good nucleophiles, the reactions of benzylamine and 1,1-diphenylmethylamine were performed in the absence of catalyst. These reactions occurred slower than those in the presence of the catalyst (Entries 5 and 7), indicating that NBS and $Br_3CCOCBr_3$ serve as catalysts for the reactions.

Table 2. *N-tert*-Butyloxycarbonylation of aliphatic amines in the presence of NBS or $Br_3CCOCBr_3$ [a]

Entry	Product		Catalyst	Yield[b] (%)	Entry	Product		Catalyst	Yield[b] (%)
1	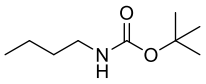	**2a**	NBS $Br_3CCOCBr_3$	98 99	10	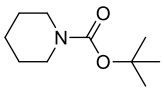	**2j**	NBS $Br_3CCOCBr_3$	81 93
2	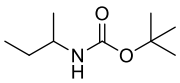	**2b**	NBS $Br_3CCOCBr_3$	90[c] 70[d]	11	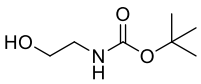	**2k**	NBS $Br_3CCOCBr_3$	99 97
3	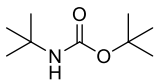	**2c**	NBS $Br_3CCOCBr_3$	66[e] 69[e]	12	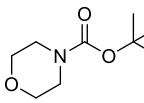	**2l**	NBS $Br_3CCOCBr_3$	93 99
4	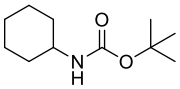	**2d**	NBS $Br_3CCOCBr_3$	quant. 86	13	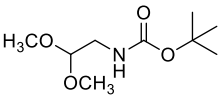	**2m**	NBS $Br_3CCOCBr_3$	98 95
5	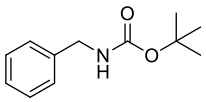	**2e**	NBS $Br_3CCOCBr_3$	80 (48)[f] quant.	14	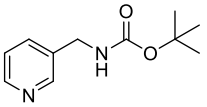	**2n**	NBS $Br_3CCOCBr_3$	97[c] 90
6	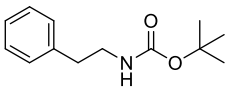	**2f**	NBS $Br_3CCOCBr_3$	99[c] 93	15	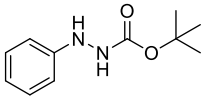	**2o**	NBS $Br_3CCOCBr_3$	87[c] 86
7	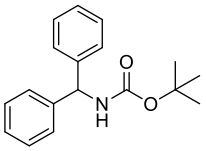	**2g**	NBS $Br_3CCOCBr_3$	75 (98)[g] (58)[f] 84 (99)[g]	16	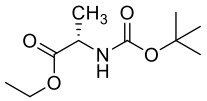	**2p**	NBS $Br_3CCOCBr_3$	82[c] 91[c]
8	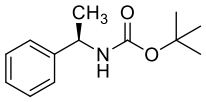	**2h**	NBS $Br_3CCOCBr_3$	99 98	17	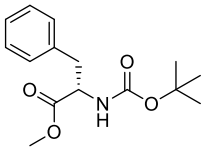	**2q**	NBS $Br_3CCOCBr_3$	85[c] 98[c]
9	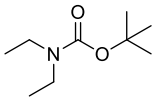	**2i**	NBS $Br_3CCOCBr_3$	62[d] 76[d]					

[a] Reaction conditions: amine (1 mmol, 1 equiv.), $(Boc)_2O$ (1 equiv.), NBS or $Br_3CCOCBr_3$ (0.10 equiv.), CH_2Cl_2 (0.2 mL), rt, 5 min (unless otherwise indicated).
[b] Isolated yield.
[c] 10 min.
[d] 1 h.
[e] 2 h.
[f] Reaction carried out without catalyst for 1 h.
[g] 30 min.

The feasibility of optimized reaction conditions was further extended to the *N-tert*-butyloxycarbonylation of several aromatic amines (Table 3).

Table 3. *N-tert*-Butyloxycarbonylation of aromatic amines in the presence of NBS or $Br_3CCOCBr_3$ [a]

Entry	Product		Catalyst	Time (h)	Yield[b] (%)	Entry	Product		Catalyst	Time (h)	Yield[b] (%)
1	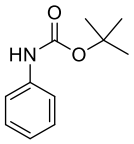	**3a**	NBS	0.5	97	8	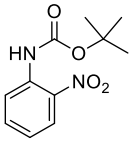	**3g**	NBS	2	18
			$Br_3CCOCBr_3$	0.25	80				$Br_3CCOCBr_3$	2	15
2	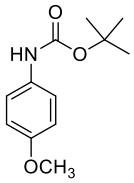	**3b**	NBS	0.25	93	9	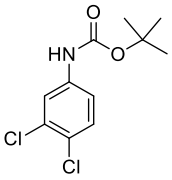	**3h**	NBS	2	78
			$Br_3CCOCBr_3$	0.25	94				$Br_3CCOCBr_3$	2	94
3	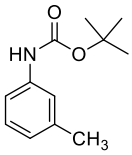	**3c**	NBS	0.25	quant.	10	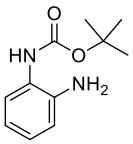	**3i**	NBS	0.25	quant. (99)[c]
			$Br_3CCOCBr_3$	0.25	95				$Br_3CCOCBr_3$	0.25	85 (98)[c]
4	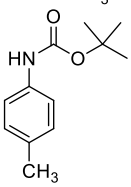	**3d**	NBS	0.25	97	11	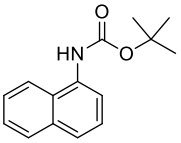	**3j**	NBS	1	97
			$Br_3CCOCBr_3$	0.25	97				$Br_3CCOCBr_3$	1	99
5	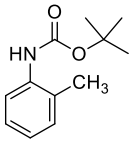	**3e**	NBS	2.5	86	12	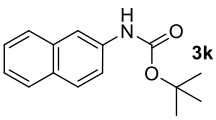	**3k**	NBS	1	98
			$Br_3CCOCBr_3$	2.5	87				$Br_3CCOCBr_3$	1	quant.
6	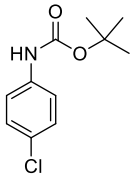	**1a**	NBS	2	96	13	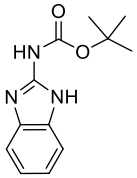	**3l**	NBS	0.5	99
			$Br_3CCOCBr_3$	2	quant.				$Br_3CCOCBr_3$	1	80
7	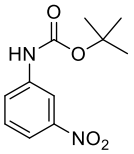	**3f**	NBS	2	61	14	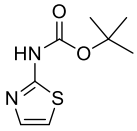	**3m**	NBS	1	76
			$Br_3CCOCBr_3$	2	72				$Br_3CCOCBr_3$	1	quant.

[a] Reaction conditions: amine (1 mmol, 1 equiv.), $(Boc)_2O$ (1 equiv.), NBS or $Br_3CCOCBr_3$ (0.10 equiv.), CH_2Cl_2 (0.2 mL), rt.
[b] Isolated yield.
[c] $(Boc)_2O$ (2 equiv.) was used and the di-*N*,*N*-Boc protected product (**3i-1**) was obtained.

Most aromatic amines required longer reaction time than aliphatic amines. Aniline and aromatic amines bearing electron-donating groups required shorter reaction times than those containing halogens or electron-withdrawing groups (Entries 1-5 *vs*. 6 and 9 *vs*. 7 and 8). Unfortunately, the steric effect of *ortho*-nitro substitutions dramatically affected the reactivity, affording the desired products in low yields (Entry 8). Nevertheless, in the case of 2-methylaniline, the corresponding products could be achieved in good yields by prolonging the reaction time (Entry 5). Under the same

conditions, 1,2-diaminobenzene was successfully converted to the corresponding mono *N*-Boc protected products, whereas di-*N*,*N*-Boc protected products were obtained by employing 2 equivalents of $(Boc)_2O$ (Entry 10). α- and β-Naphthalenes could be transformed into the *N*-Boc products in almost quantitative yields (Entries 11 and 12). Notably, the chemoselectivity was observed from the reaction of benzylimidazole and 2-aminothiazole, heteroaromatic amine, yielding the corresponding *N*-Boc products in good to excellent yields (Entries 13 and 14).

To investigate the reaction chemoselectivity with amino groups with different electronic environments, a competitive reaction between aromatic and aliphatic amines was performed using 4-aminophenethylamine (**4**) as a model compound (Table 4).

Table 4. Chemoselective *N*-*tert*-butyloxycarbonylation of amine using a competitive reaction between aromatic and aliphatic amines

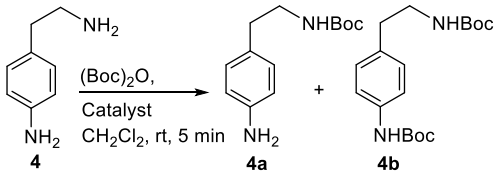

Entry	$(Boc)_2O$ (equiv.)	Catalyst	Yield (%)[b]	
			4a	**4b**
1	1	NBS	85	-
2	1	$Br_3CCOCBr_3$	97	-
3	2	NBS	-	86
4	2	$Br_3CCOCBr_3$	-	91

[a] Reaction conditions: amine (1 mmol, 1 equiv.), $(Boc)_2O$, NBS or $Br_3CCOCBr_3$ (0.10 equiv.), CH_2Cl_2 (0.2 mL), rt.
[b] Isolated yield.

When 4-aminophenethylamine (1 mmol) treated with $(Boc)_2O$ (1 mmol) for 5 min, $Br_3CCOCBr_3$ displayed significantly higher reactivity over NBS towards the *N*-Boc protection at the alkyl amino group, furnishing (2-(4-aminophenyl)ethyl)-carbamic acid *tert*-butyl ester (**4a**) as the major product in 97% and 85% yields, respectively (Entries 1 and 2). These results were in good agreement with prior observations that the reactivity of aliphatic amines was higher than that of aromatic amines due to their increased nucleophilicity. When $(Boc)_2O$ (2 mmol) was used with NBS or $Br_3CCOCBr_3$, the reactions gave only di-*N*,*N*-Boc products (**4b**) in 86% and 91% yields, respectively (Entries 3 and 4).

To explore a reaction mechanism, the preliminary experiments were performed using IR spectroscopy and the results are presented in IR spect.

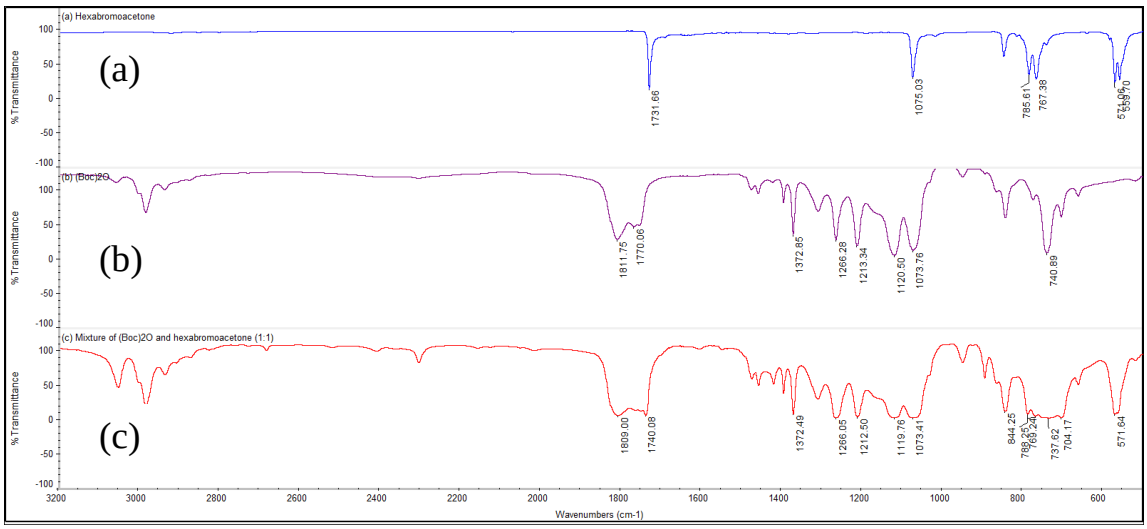

Figure 1. IR spectrum (in CH_2Cl_2 solution) of (a) $Br_3CCOCBr_3$; (b) $(Boc)_2O$ and (c) the mixture of $(Boc)_2O$ and $Br_3CCOCBr_3$ (1:1)

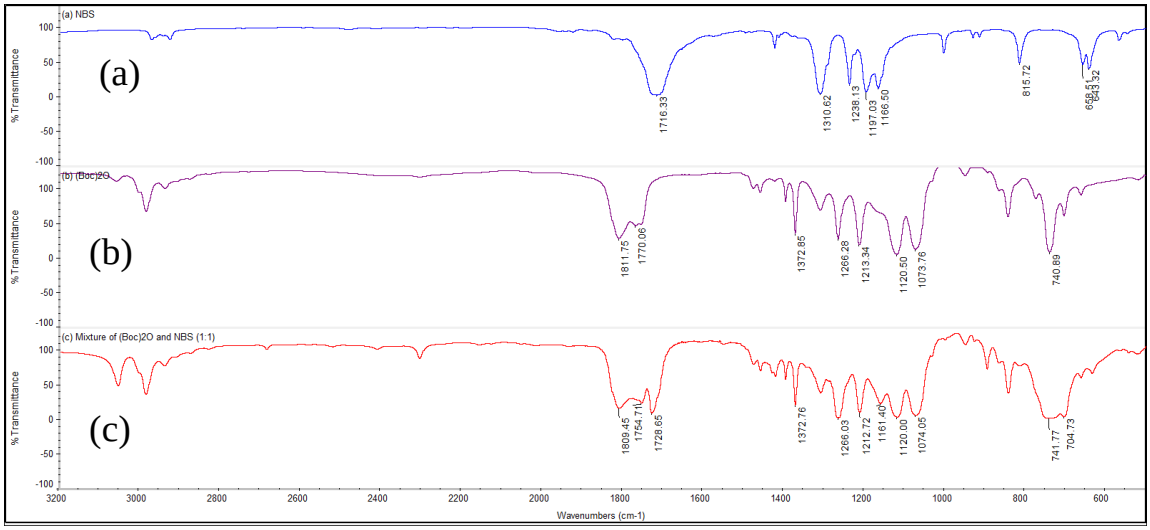

Figure 2. IR spectrum (in CH_2Cl_2 solution) of (a) NBS; (b) $(Boc)_2O$ and (c) the mixture of $(Boc)_2O$ and NBS (1:1)

The IR spectrum of an equimolar mixture of $(Boc)_2O$ and $Br_3CCOCBr_3$ revealed the frequency assigned to the C=O stretching vibration at 1809.00 cm^{-1}, while the C=O stretching frequency of free $(Boc)_2O$ presented at 1811.75 and 1770.06 cm^{-1} (see IR spectrum 1). The similar result was also observed from the IR spectrum of the mixture of $(Boc)_2O$ and NBS showing the frequencies of the C=O stretching vibration at

1809.45 and 1754.71 cm^{-1} (see IR spectrum 2). The shift of C=O stretching frequencies is probably caused by the coordination of $(Boc)_2O$ with $Br_3CCOCBr_3$ (or NBS), resulting in the disappearance of β-diketone moiety of $(Boc)_2O$ in **TS-1** (Scheme 1).[25, 47] A proposed mechanism is depicted in Scheme 1. Similar to the mechanism of the iodine-catalyzed reactions,[25] a carbonyl carbon of $(Boc)_2O$ is initially activated by donation of an oxygen lone pair to a partially positively charged bromine atom of $Br_3CCOCBr_3$ (or NBS) to generate **TS-1**. Then, the nucleophilic attack by the amine on the electrophilic carbonyl carbon of **TS-1** produces **TS-2**, which decomposes to give the desired *N*-Boc-protected amine together with the formation of *tert*-butanol and carbon dioxide as by-products.

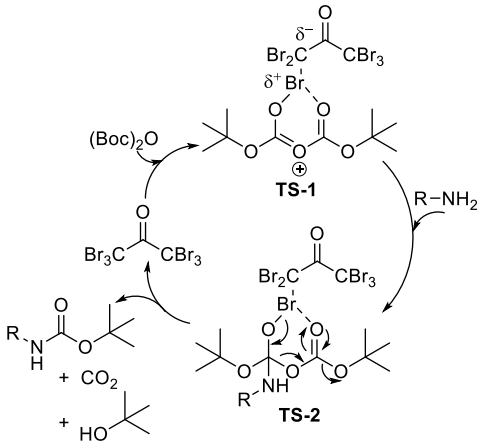

Scheme 1 Proposed mechanism

5. Conclusion

Synthetic cluvenone analogues **CR135** and **CR142**, containing a triphenylphosphonium group at the A ring were found to be the potent antimalarial activity against *P. falciparum* parasites with as low as ca.10 nM. The caged motif is important for antimalarial activity. These findings produced new antimalarial drug candidates and a significant impact to public health.

A mild and facile methodology for the *N*-*tert*-butyloxycarbonylation of amines utilizing NBS and $Br_3CCOCBr_3$ as catalysts was explored. Aliphatic and aromatic amines could be chemoselectively converted to *N*-Boc protected products in good to excellent yields with short reaction times at room temperature.

6. References

1. Chantarasriwong, O., Batova, A., Chavasiri, W.,Theodorakis, E. A. *Chem. Eur. J.* **2010**, 16, 9944.
2. WHO (ed) (2015) *World Malaria* Report.
3. Crompton, P. D.; Moebius, J.; Portugal, S.; Waisberg, M.; Hart, G.; Garver, L. S.; Miller, L. H.; Barillas-Mury, C.; and Pierce, S. K. *Annu. Rev. Immunol.*, **2014**, *32*, 157.
4. White, N. J.; Pukrittayakamee, S.; Hien, T. T.; Faiz, M. A.; Mokuolu, O. A.; Dondorp, A. M. Lancet., **2014**, *383*, 723.
5. Ashley, E. A.; Dhorda, M.; Fairhurst, R. M.; Amaratunga, C.; Lim, P.; Suon, S.; Sreng, S.; Anderson, J. M.; Mao, S.; Sam, B.; Sopha, C.; Chuor, C. M.; Nguon, C.; Sovannaroth, S.; Pukrittayakamee, S.; Jittamala, P.; Chotivanich, K.; Chutasmit, K.; Suchatsoonthorn, C.; Runcharoen, R.; Hien, T. T.; Thuy-Nhien, N. T.; Thanh, N. V.; Phu, N. H.; Htut, Y.; Han, K.-T.; Aye, K. H.; Mokuolu, O. A.; Olaosebikan, R. R.; Folaranmi, O. O.; Mayxay, M.; Khanthavong, M.; Hongvanthong, B.; Newton, P. N.; Onyamboko, M. A.; Fanello, C. I.; Tshefu, A. K.; Mishra, N.; Valecha, N.; Phyo, A. P.; Nosten, F.; Yi, P.; Tripura, R.; Borrmann, S.; Bashraheil, M.; Peshu, J.; Faiz, M. A.; Ghose, A.; Hossain, M. A.; Samad, R.; Rahman, M. R.; Hasan, M. M.; Islam, A.; Miotto, O.; Amato, R.; MacInnis, B.; Stalker, J.; Kwiatkowski, D. P.; Bozdech, Z.; Jeeyapant, A.; Cheah, P. Y.; Sakulthaew , T.; Chalk , J.; Intharabut , B.; Silamut , K.; Lee , S. J.; Vihokhern, B.; Kunasol, C.; Imwong, M.; Tarning, J.; Taylor, W. J.; Yeung, S.; Woodrow, C. J.; Flegg, J. A.; Das, D.; Smith, J.; Venkatesan, M.; Plowe, C. V.; Stepniewska, K.; Guerin, P. J.; Dondorp, A. M.; Day, N. P.; White, *N. Engl. J. Med.*, **2014**, 371, 411.
6. Straimer, J.; Gnädig, N. F.; Witkowski, B.; Amaratunga, C.; Duru, V.; Ramadani, A. P.; Dacheux, M.; Khim, N.; Zhang, L.; Lam, S.; Gregory, P. D.; Urnov, F. D.; Mercereau-Puijalon, O.; Benoit-Vical, F.; Fairhurst, R. M.; Ménard, D.; Fidock, D. A. *Science* **2015**, *347*, 428.
7. Mok, S.; Ashley, E. A.; Ferreira, P. E.; Zhu, L.; Lin, Z.; Yeo, T.; Chotivanich, K.; Imwong, M.; Pukrittayakamee, S.; Dhorda, M.; Nguon, C.; Lim, P.; Amaratunga, C.; Suon, S.; Hien, T. T.; Htut, Y.; Faiz, M. A.; Onyamboko, M. A.; Mayxay, M.; Newton, P. N.; Tripura, R.; Woodrow, C. J.; Miotto, O.; Kwiatkowski, D. P.; Nosten, F.; Day, N. P. J.; Preiser, P. R.; White, N. J.; Dondorp, A. M.; Fairhurst, R. M.; Bozdech, Z. *Science* **2015**, *347*, 431.
8. Greene, T. W. W., P. G. M. *In Protecting Group in Organic Synthesis*; John Wiley and Sons: New York, 1999.
9. Pope, B. M. Y., X.; Tarbell, D. S. *Org. Synth. Coll.* **1988**, *VI*, 418.
10. Basel, Y.; Hassner, A. *J. Org. Chem.* **2000**, *65*, 6368.
11. Swenson, R. E.; Sowin, T. J.; Zhang, H. Q. *J. Org. Chem.* **2002**, *67*, 9182.
12. B. Harris, R.; B. Wilson, I. *Tetrahedron Lett*. **1983**, *24*, 231.
13. Kelly, T. A.; McNeil, D. W. *Tetrahedron Lett.* **1994**, *35*, 9003.
14. Basel, Y.; Hassner, A. *J. Org. Chem.* **2000**, *65*, 6368.
15. Sharma, G. V. M.; Janardhan Reddy, J.; Sree Lakshmi, P.; Radha Krishna, P. *Tetrahedron Lett.* **2004**, *45*, 6963.
16. Bartoli, G. B., M.; Locatelli, M.; Marcantoni, E.; Massaccesi, M.; Melchiorre, P.; Sambri, L. *Synlett* **2004**, 1794.
17. Heydari, A.; Hosseini, S. E. *Adv. Synth. Catal.* **2005**, *347*, 1929.
18. Rajanna, K. C. *Synth. Commun.* **2011**, *41*, 715.

19. Chankeshwara, S. V.; Chakraborti, A. K. *Tetrahedron Lett.* **2006**, *47*, 1087.
20. Suryakiran, N.; Prabhakar, P.; Reddy, T. S.; Rajesh, K.; Venkateswarlu, Y. *Tetrahedron Lett*. **2006**, *47*, 8039.
21. Suryakiran, N.; Prabhakar, P.; Reddy, T. S.; Srinivasulu, M.; Swamy, N. R.; Venkateswarlu, Y. *J. Mol. Catal. A: Chem.* **2007**, *264*, 40.
22. Chankeshwara, S. V.; Chakraborti, A. K. *Synthesis* **2006**, 2784.
23. Inahashi, N.; Matsumiya, A.; Sato, T. *Synlett* **2008**, 294.
24. Varala, R.; Nuvula, S.; Adapa, S. R. *J. Org. Chem.* **2006**, *71*, 8283.
25. Shailaja, M.; Manjula, A.; Rao, B. V. *Synth. Commun.* **2011**, *41*, 2073.
26. Heydari, A.; Khaksar, S.; Tajbakhsh, M. *Synthesis* **2008**, 3126.
27. Khaksar, S.; Heydari, A.; Tajbakhsh, M.; Vahdat, S. M. *Tetrahedron Lett.* **2008**, *49*, 3527.
28. Khaksar, S.; Vahdat, S. M.; Tajbakhsh, M.; Jahani, F.; Heydari, A. *Tetrahedron Lett*. **2010**, *51*, 6388.
29. Jahani, F.; Tajbakhsh, M.; Golchoubian, H.; Khaksar, S. *Tetrahedron Lett.* **2011**, *52*, 1260.
30. Upadhyaya, D. J.; Barge, A.; Stefania, R.; Cravotto, G. *Tetrahedron Lett.* **2007**, *48*, 8318.
31. Shirini, F.; Zolfigol, M. A.; Abedini, M. *J. Iran. Chem. Soc*. **2010**, *7*, 603.
32. Shirini, F.; Khaligh, N. G. *Monatsh. Chem.* **2012**, *143*, 631.
33. Heydari, A.; Shiroodi, R. K.; Hamadi, H.; Esfandyari, M.; Pourayoubi, M. *Tetrahedron Lett.* **2007**, *48*, 5865.
34. Chankeshwara, S. V.; Chakraborti, A. K. *J. Mol. Catal. A: Chem.* **2006**, *253*, 198.
35. Kumar, K. S.; Iqbal, J.; Pal, M. *Tetrahedron Lett.* **2009**, *50*, 6244.
36. Das, B.; Venkateswarlu, K.; Krishnaiah, M.; Holla, H. *Tetrahedron Lett.* **2006**, *47*, 7551.
37. Atghia, S. V.; Sarvi Beigbaghlou, S. *J. Organomet. Chem.* **2013**, *745-746*, 42.
38. Shirini, F.; Mamaghani, M.; Atghia, S. V. *Catal.* Commun. **2011**, *12*, 1088.
39. Veisi, H.; Sedrpoushan, A.; Ghazizadeh, H.; Hemmati, S. *Res. Chem. Intermed*. **2016**, *42*, 1451.
40. Karmakar, B.; Banerji, J. *Tetrahedron Lett*. **2010**, *51*, 3855.
41. Chakraborti, A. K.; Chankeshwara, S. V. *Org. Biomol. Chem.* **2006**, *4*, 2769.
42. Khaligh, N. G.; Hazarkhani, H. *Monatsh. Chem.* **2014**, *145*, 1975.
43. Shirini, F.; Atghia, S. V.; Jirdehi, M. G. *Chin. Chem. Lett.* **2013**, *24*, 34.
44. Zolfigol, M. A.; Moosavi-Zare, A. R.; Moosavi, P.; Khakyzadeh, V.; Zare, A. *C. R. Chim.* **2013**, *16*, 962.
45. Chaskar, A.; Yewale, S.; Langi, B.; Deokar, H. *J. Korean Chem. Soc.* **2009**, *53*, 422.
46. Sunitha, S.; Kanjilal, S.; Reddy, P. S.; Prasad, R. B. N. *Tetrahedron Lett.* **2008**, *49*, 2527.
47. Akbari, J.; Heydari, A.; Ma'mani, L.; Hosseini, S. H. *C. R. Chim.* **2010**, *13*, 544.
48. Karimian, S.; Tajik, H. *Chin. Chem. Lett*. **2014**, *25*, 218.
49. Shirini, F.; Jolodar, O. G.; Seddighi, M.; Borujeni, H. T. *RSC Adv*. **2015**, *5*, 19790.
50. Sarkar, A.; Roy, S. R.; Parikh, N.; Chakraborti, A. K. *J. Org. Chem.* **2011**, *76*, 7132.
51. Shirini, F.; Khaligh, N. G. *J. Mol. Liq.* **2013**, *177*, 386.
52. Majumdar, S.; De, J.; Chakraborty, A.; Maiti, D. K. *RSC Adv.* **2014**, *4*, 24544.
53. Reddy, M. S.; Narender, M.; Nageswar, Y. V. D.; Rao, K. R. *Synlett* **2006**, 1110.
54. Chankeshwara, S. V.; Chakraborti, A. K. *Org. Lett*. **2006**, *8*, 3259.
55. Vilaivan, T. *Tetrahedron Lett*. **2006**, *47*, 6739.

56. Siddaiah, V.; Basha, G. M.; Rao, G. P.; Prasad, U. V.; Rao, R. S. *Chem. Lett.* **2010**, *39*, 1127.
57. Zeng, H.; Li, Y.; Shao, H. *Synth. Commun.* **2012**, *42*, 25.
58. Jia, X.; Huang, Q.; Li, J.; Li, S.; Yang, Q. *Synlett* **2007**, *2007*, 0806.
59. Dighe, S. N.; Jadhav, H. R. *Tetrahedron Lett.* **2012**, *53*, 5803.
60. Nardi, M.; Cano, N. H.; Costanzo, P.; Oliverio, M.; Sindona, G.; Procopio, A. *RSC Adv.* **2015**, *5*, 18751.
61. Tongkate, P.; Pluempanupat, W.; Chavasiri, W. *Tetrahedron Lett.* **2008**, *49*, 1146.
62. Menezes, F. G.; Kolling, R.; Bortoluzzi, A. J.; Gallardo, H.; Zucco, C. *Tetrahedron Lett.* **2009**, *50*, 2559.
63. Guinet, F.; Dvorak, J. A.; Fujioka, H.; Keister, D. B.; Muratova, O.; Kaslow, D. C.; Aikawa, M.; Vaidya, A. B.; Wellems, T. E. *The Journal of Cell Biology* **1996**, *135*, 269.
64. Alin, M. H.; Bjorkman, A.; Ashton, M. *Trans R. Soc. Trop. Med. Hyg.*, **1990**, *84*, 635.
65. Theodoraki, M. A.; Rezende Jr., C. O.; Chantarasriwong, O.; Corben, A. D.; Theodorakis, E. A.; Alpaugh, M. L. *Oncotarget* **2015**, *6*, 21255.
66. Keller, L.; Beaumont, S.; Liu, J.-M.; Thoret, S.; Bignon, J. S.; Wdzieczak-Bakala, J.; Dauban, P.; Dodd, R. H. *Journal of Medicinal Chemistry* **2008**, *51*, 3414.
67. Saito, Y.; Ouchi, H.; Takahata, H. *Tetrahedron* **2006**, *62*, 11599.

Output จากโครงการวิจัยที่ได้รับทุนจาก สกว.

ผลงานตีพิมพ์ในวารสารวิชาการนานาชาติ 2 เรื่อง คือ

1. Oraphin Chantarasriwong,* Banphot Jiangchareon, Christian Kurnia Putra, Winai Suwankrua, Warinthorn Chavasiri "NBS and $Br_3CCOCBr_3$ as highly efficient catalysts for the chemoselective *N*-tert-butyloxycarbonylation of amines" Tetrahedron Letters, **2016**, *57*, 4807–4811. (Science Citation Index (Web of Science), Impact factor (2015): 2.347)
2. Hangjun Ke, Joanne M. Morrisey, Shiwei Qu, Oraphin Chantarasriwong, Michael W. Mather, Emmanuel A. Theodorakis and Akhil B. Vaidya. Caged Garcinia xanthones: a novel chemical scaffold with potent antimalarial activity. Antimicrobial Agents and Chemotherapy, **2016**, (Science Citation Index Expanded (Web of Science), Impact factor (2015): 4.415) (In press)

ข้อเสนอแนะสำหรับงานวิจัยในอนาคต

ทุนนักวิจัยรุ่นใหม่เป็นทุนที่ดีมาก เป็นทุนที่ให้โอกาสนักวิจัยรุ่นใหม่ได้ตั้งตัวในการทำการวิจัยและเป็นแรงกระตุ้นอย่างในการผลิตผลงานวิจัย โดยเฉพาะการได้ผลงานตีพิมพ์ในวารสารวิชาการนานาชาติ ที่ผู้วิจัยเป็นผู้เขียนหลัก จึงหากมีโอกาสควรเพิ่มจำนวนทุนวิจัยนี้ต่อไป

Appendix

Tetrahedron Letters 57 (2016) 4807–4811

Contents lists available at ScienceDirect

Tetrahedron Letters

journal homepage: www.elsevier.com/locate/tetlet

NBS and $Br_3CCOCBr_3$ as highly efficient catalysts for the chemoselective *N-tert*-butyloxycarbonylation of amines

Oraphin Chantarasriwong [a,*], Banphot Jiangchareon [a], Christian Kurnia Putra [a], Winai Suwankrua [a], Warinthorn Chavasiri [b]

[a] Department of Chemistry, Faculty of Science, King Mongkut's University of Technology Thonburi, 126 Pracha Uthit Rd., Bang Mod, Thung Khru, Bangkok 10140, Thailand
[b] Department of Chemistry, Faculty of Science, Chulalongkorn University, Bangkok 10330, Thailand

ARTICLE INFO

Article history:
Received 1 July 2016
Revised 29 August 2016
Accepted 14 September 2016
Available online 17 September 2016

Keywords:
N-tert-Butyloxycarbonylation
di-*tert*-Butyl dicarbonate
N-Bromosuccinimide
Hexabromoacetone

ABSTRACT

N-Bromosuccinimide (NBS) and hexabromoacetone ($Br_3CCOCBr_3$) were found to be new and efficient catalysts for the chemoselective *N-tert*-butyloxycarbonylation of aliphatic and aromatic amines. This novel, simple, and effective method for the preparation of *N*-Boc protected products proceeds in good to excellent yields with short reaction times at room temperature.

The protection of amino groups plays a significant role in the multi-step synthesis of peptides and nitrogen-containing pharmaceuticals.[1] The most frequently employed amine protection methods involve the formation of an *N-tert*-butyloxycarbonyl (*N*-Boc) group due to its stability toward catalytic hydrogenation, base and nucleophilic attack, as well as the ease of removal under mild acidic conditions.[1]

The *N*-Boc group is frequently introduced by the treatment of amines with di-*tert*-butyl dicarbonate [$(Boc)_2O$] because of its low price, commercial availability, stability, and efficiency.[2] Organic and inorganic bases, including DMAP,[3] NaOH,[4] NH_2OH,[5] NaHMDS,[6] and K_2CO_3,[1] have been used as reagents or catalysts, however these methods present certain disadvantages including long reaction times, use of an excess of reagents, unsatisfactory yields, and the formation of isocyanates, ureas, or *N*,*N*-di-Boc derivatives as by-products.[3]

Alternatively, methods involving Lewis or Brønsted acid catalysts, such as $ZrCl_4$,[7] $Zn(ClO_4)_2{\cdot}6H_2O$,[8] $LiClO_4$,[9] $FeCl_3$,[10] $Cu(BF_4)_2{\cdot}xH_2O$,[11] $La(NO_3)_3{\cdot}6H_2O$,[12] $Bi(NO_3)_3{\cdot}5H_2O$,[13] $InCl_3$, $InBr_3$,[14] CsF,[15] I_2,[16] Me_2SBr_2,[17] $(CF_3)_2CHOH$,[18] thiourea,[19] thioglycoluril,[20] guanidine hydrochloride,[21] sulfamic acid,[22] saccharin sulfonic acid,[23] and succinimide sulfonic acid have been reported.[24] There are also reports regarding the *N-tert*-butyloxycarbonylation of amines using heterogeneous catalysts, including $H_3PW_{12}O_{40}$,[25] montmorillonite K10 or KSF,[26] amberlyst-15,[27] sulfonic acid-functionalized silica,[28] sulfonic acid-functionalized nanoporous titania,[29] sulfonic acid-functionalized ordered nanoporous Na^+-montmorillonite,[30] mesoporous silica phenylsulfonic acid,[31] tungstophosphoric acid-doped mesoporous silica,[32] $HClO_4$-SiO_2,[33] poly(4-vinylpyridinium) perchlorate,[34] nano-TiO_2-$HClO_4$,[35] nano-Fe_3O_4,[36] and indion 190 resin.[37] Acidic ionic liquids, such as [(HMIm)BF_4],[38] [TMG][Ac],[39] [Py][OTf],[40] [H-Suc]HSO_4,[41] an 1-alkyl-3-methylimidazolium-based ionic liquid,[42] 1,3-disulfonic acid imidazolium hydrogen sulfate,[43] and imidazolium trifluoroacetate,[44] have also been used as catalysts for the *N-tert*-butyloxycarbonylation of amines. Other procedures have also been reported, including the use of β-cyclodextrin,[45] catalyst-free reactions in water,[46] ethanol,[47] and polyethylene glycols[48,49] as well as solvent-free conditions with and without microwave irradiation.[50–52] Although these methodologies provide a marked improvement over past methods, some still possess drawbacks such as moisture-sensitive reagents, prolonged reaction times, time consuming work-up procedures, harsh reaction conditions, and tedious steps needed for the preparation of reagents/catalysts. In addition, some methods require large amounts of Lewis acid that affects the reaction rate due to the deactivation of amines. As a result, the development of new, facile, and effective methods for the *N-tert*-butyloxycarbonylation of amines still represents a desirable goal.

N-Bromosuccinimide (NBS) is a widely known reagent or catalyst for numerous organic transformations. In recent years, hexabromoacetone ($Br_3CCOCBr_3$) has also received interest as a

* Corresponding author. Tel.: +66 2 470 9552; fax: +66 2 470 8843.
E-mail address: oraphin.cha@kmutt.ac.th (O. Chantarasriwong).

http://dx.doi.org/10.1016/j.tetlet.2016.09.052
0040-4039/

Table 1
Effect of catalyst type and amount on the *N-tert*-butyloxycarbonylation of 4-chloroaniline (**1**)

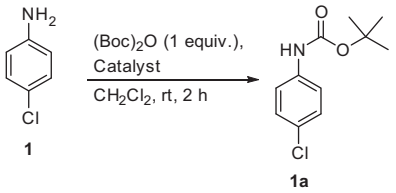

Entry	Catalyst		Yield[a] (%)
	Type	mol%	
1	None	–	35[b]
2	CBr_4	10	65
3	$CHBr_3$	10	57
4	NBS	10	96
5	NBS	5	43
6	$Br_3CCOCBr_3$	10	quant.
7	$Br_3CCOCBr_3$	5	54
8	HBr	10	22[b]

[a] Isolated yield.
[b] 24 h.

brominating agent for the synthesis of alkyl bromides[53] and acid bromides[54] and as a tribromoacetylating agent for alcohols and amines.[54] To the best of our knowledge, few reports exist concerning the use of $Br_3CCOCBr_3$ for organic reactions[53,54] and there are no reports on the utilization of NBS and $Br_3CCOCBr_3$ as catalysts for the *N-tert*-butyloxycarbonylation of amines. Therefore, we describe herein the use of NBS and $Br_3CCOCBr_3$ as catalysts in the *N-tert*-butyloxycarbonylation of amines under mild reaction conditions.

The effect of catalyst type and amount was initially investigated using 4-chloroaniline (**1**, 1 mmol) as a model substrate for the reaction with $(Boc)_2O$ (1 mmol) in CH_2Cl_2 (0.2 mL) at room temperature (Table 1).

In the absence of catalyst, the *N*-Boc protected product was isolated in only 35% yield after 24 h (Entry 1). To improve the yield, different catalysts containing bromine atoms were employed. A moderate yield of the desired product was achieved when carrying out the reaction with CBr_4 and $CHBr_3$ (57–65%, Entries 2 and 3). The use of 10 mol% NBS led to an almost quantitative yield of the desired product within 2 h at room temperature (Entry 4). $Br_3CCOCBr_3$ also produced the desired product quantitatively, whereas HBr gave the desired product in 22% yield after 24 h

Table 2
N-tert-Butyloxycarbonylation of aliphatic amines in the presence of NBS or $Br_3CCOCBr_3$[a]

Entry	Product	Catalyst	Yield[b] (%)	Entry	Product	Catalyst	Yield[b] (%)
1	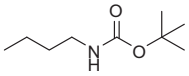 **2a**	NBS $Br_3CCOCBr_3$	98 99	10	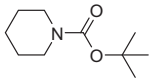 **2j**	NBS $Br_3CCOCBr_3$	81 93
2	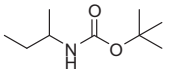 **2b**	NBS $Br_3CCOCBr_3$	90[c] 70[d]	11	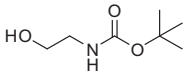 **2k**	NBS $Br_3CCOCBr_3$	99 97
3	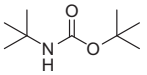 **2c**	NBS $Br_3CCOCBr_3$	66[e] 69[e]	12	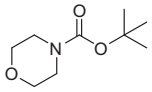 **2l**	NBS $Br_3CCOCBr_3$	93 99
4	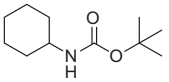 **2d**	NBS $Br_3CCOCBr_3$	quant. 86	13	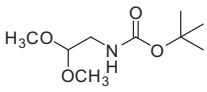 **2m**	NBS $Br_3CCOCBr_3$	98 95
5	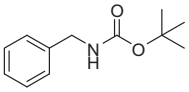 **2e**	NBS $Br_3CCOCBr_3$	80 (48)[f] quant.	14	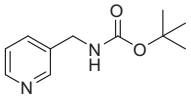 **2n**	NBS $Br_3CCOCBr_3$	97[c] 90
6	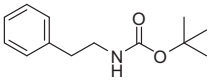 **2f**	NBS $Br_3CCOCBr_3$	99[c] 93	15	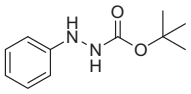 **2o**	NBS $Br_3CCOCBr_3$	87[c] 86
7	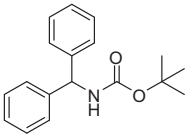 **2g**	NBS $Br_3CCOCBr_3$	75 (98)[g] (58)[f] 84 (99)[g]	16	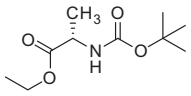 **2p**	NBS $Br_3CCOCBr_3$	82[c] 91[c]
8	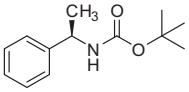 **2h**	NBS $Br_3CCOCBr_3$	99 98	17	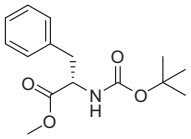 **2q**	NBS $Br_3CCOCBr_3$	85[c] 98[c]
9	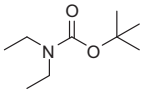 **2i**	NBS $Br_3CCOCBr_3$	62[d] 76[d]				

[a] Reaction conditions: amine (1 mmol, 1 equiv), $(Boc)_2O$ (1 equiv), NBS or $Br_3CCOCBr_3$ (0.10 equiv), CH_2Cl_2 (0.2 mL), rt, 5 min (unless otherwise indicated).
[b] Isolated yield.
[c] 10 min.
[d] 1 h.
[e] 2 h.
[f] Reaction carried out without catalyst for 1 h.
[g] 30 min.

Table 3
N-tert-Butyloxycarbonylation of aromatic amines in the presence of NBS or $Br_3CCOCBr_3$[a]

Entry	Product	Catalyst	Time (h)	Yield[b] (%)	Entry	Product	Catalyst	Time (h)	Yield[b] (%)
1	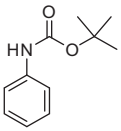 **3a**	NBS $Br_3CCOCBr_3$	0.5 0.25	97 80	8	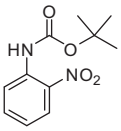 **3g**	NBS $Br_3CCOCBr_3$	2 2	18 15
2	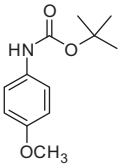 **3b**	NBS $Br_3CCOCBr_3$	0.25 0.25	93 94	9	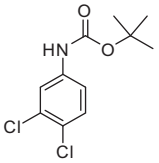 **3h**	NBS $Br_3CCOCBr_3$	2 2	78 94
3	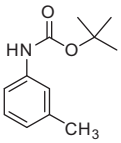 **3c**	NBS $Br_3CCOCBr_3$	0.25 0.25	quant. 95	10	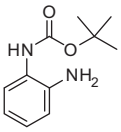 **3i**	NBS $Br_3CCOCBr_3$	0.25 0.25	quant. (99)[c] 85 (98)[c]
4	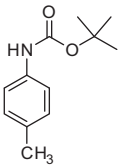 **3d**	NBS $Br_3CCOCBr_3$	0.25 0.25	97 97	11	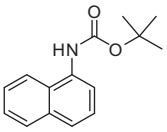 **3j**	NBS $Br_3CCOCBr_3$	1 1	97 99
5	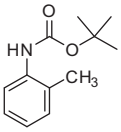 **3e**	NBS $Br_3CCOCBr_3$	2.5 2.5	86 87	12	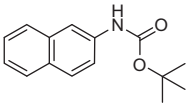 **3k**	NBS $Br_3CCOCBr_3$	1 1	98 quant.
6	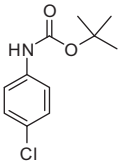 **1a**	NBS $Br_3CCOCBr_3$	2 2	96 quant.	13	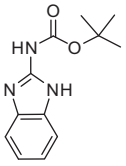 **3l**	NBS $Br_3CCOCBr_3$	0.5 1	99 80
7	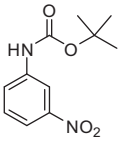 **3f**	NBS $Br_3CCOCBr_3$	2 2	61 72	14	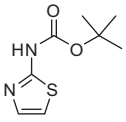 **3m**	NBS $Br_3CCOCBr_3$	1 1	76 quant.

[a] Reaction conditions: amine (1 mmol, 1 equiv), $(Boc)_2O$ (1 equiv), NBS or $Br_3CCOCBr_3$ (0.10 equiv), CH_2Cl_2 (0.2 mL), rt.
[b] Isolated yield.
[c] $(Boc)_2O$ (2 equiv) was used and the di-*N*,*N*-Boc protected product (**3i–1**) was obtained.

(Entries 6 and 8). With the intention of using the lowest possible catalyst loading, the amount of NBS and $Br_3CCOCBr_3$ were reduced to 5 mol%, resulting in significant decreases in yield to 43% and 54%, respectively (Entries 5 and 7). These results indicated that 10 mol% of NBS and $Br_3CCOCBr_3$ were optimal for the *N-tert*-butyloxycarbonylation of amines with $(Boc)_2O$.

With the optimal reaction conditions established, the limitations and generality of the method were examined by the *N-tert*-butyloxycarbonylation of various aliphatic amines (Table 2).

The reaction of primary and secondary aliphatic amines with $(Boc)_2O$ in the presence of 10 mol% NBS or $Br_3CCOCBr_3$ proceeded quickly. The *N*-Boc protected products were isolated in good to excellent yields (62–100%, Entries 1–17) within 5 min to 2 h without the formation of by-products such as urea and isocyanate derivatives. The steric hindrance of the amines had an effect on the reaction rates and/or product yields. For example, the sterically hindered *tert*-butyl amine required longer reaction times than *n*-butylamine and *sec*-butylamine to achieve good product yields (Entries 1 and 2 vs 3). In the case of the chiral amine (*R*)-(+)-1-phenylethylamine, both NBS and $Br_3CCOCBr_3$ gave the optically pure *N*-Boc protected product (as determined by the optical rotation and comparison with literature values)[55] in nearly quantitative yield after 5 min (Entry 8). Ethanolamine, morpholine, and dimethylaminoacetal were chemoselectively converted into the corresponding *N*-Boc protected products in near quantitative yields without any *O*-Boc protected products formed (Entries 11–13). Highly chemoselective reactions were also performed using amines containing two different types of amino groups, such as 3-picolylamine and phenylhydrazine, where only primary amino groups were protected to give the corresponding mono *N*-Boc products in excellent yields (Entries 14–15). In the case of amino acid esters, L-alanine ethyl ester and L-phenylalanine methyl ester were converted to the corresponding *N*-Boc products in good to excellent yields (82–98%, Entries 16 and 17) without racemization

Table 4
Chemoselective *N*-*tert*-butyloxycarbonylation of amine using a competitive reaction between aromatic and aliphatic amines[a]

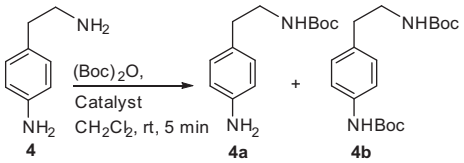

Entry	$(Boc)_2O$ (equiv)	Catalyst	Yield (%)[b]	
			4a	**4b**
1	1	NBS	85	–
2	1	$Br_3CCOCBr_3$	97	–
3	2	NBS	–	86
4	2	$Br_3CCOCBr_3$	–	91

[a] Reaction conditions: amine (1 mmol, 1 equiv), $(Boc)_2O$, NBS or $Br_3CCOCBr_3$ (0.10 equiv), CH_2Cl_2 (0.2 mL), rt.
[b] Isolated yield.

(as determined by the optical rotation and comparison with literature values).[46,56] Since primary aliphatic amines are very good nucleophiles, the reactions of benzylamine and 1,1-diphenylmethylamine were also performed in the absence of catalyst. These reactions proceeded slower than those in the presence of NBS and $Br_3CCOCBr_3$, indicating that these reagents serve as catalysts (Entries 5 and 7).

The feasibility of optimized reaction conditions was further extended to the *N*-*tert*-butyloxycarbonylation of several aromatic amines (Table 3).

Most aromatic amines required longer reaction times than aliphatic amines. Aniline and aromatic amines bearing electron-donating groups required shorter reaction times than those containing halogens or electron-withdrawing groups (Entries 1–5 vs 6 and 9 vs 7 and 8). Unfortunately, the steric effect of *ortho*-nitro substitutions dramatically affected the reactivity, affording the desired products in low yields (Entry 8). Nevertheless, in the case of 2-methylaniline, the corresponding products could be achieved in good yields by prolonging the reaction time (Entry 5). Under the same conditions, 1,2-diaminobenzene was successfully converted to the corresponding mono *N*-Boc protected products, whereas di-*N*,*N*-Boc protected products were obtained by employing 2 equivalents of $(Boc)_2O$ (Entry 10). α- and β-naphthalenes could be transformed into the corresponding *N*-Boc products in almost quantitative yields (Entries 11 and 12). Notably, chemoselectivity was observed in the reactions of benzylimidazole and 2-aminothiazole, yielding the corresponding *N*-Boc products in good to excellent yields (Entries 13 and 14).

To investigate the reaction chemoselectivity with amino groups containing different electronic environments, a competitive reaction between aromatic and aliphatic amines was performed using 4-aminophenethylamine (**4**) as a model compound (Table 4).

When 4-aminophenethylamine (1 mmol) was treated with $(Boc)_2O$ (1 mmol) for 5 min, $Br_3CCOCBr_3$ displayed significantly higher reactivity over NBS toward *N*-Boc protection at the alkyl amino group, furnishing (2-(4-aminophenyl)ethyl)-carbamic acid *tert*-butyl ester (**4a**) as the major product in 97% and 85% yields, respectively (Entries 1 and 2). These results were in good agreement with prior observations that the reactivity of aliphatic amines was higher than that of aromatic amines due to their increased nucleophilicity. When $(Boc)_2O$ (2 mmol) was used with NBS or $Br_3CCOCBr_3$, the reactions gave only di-*N*,*N*-Boc products (**4b**) in 86% and 91% yields, respectively (Entries 3 and 4).

To explore a reaction mechanism, preliminary experiments were performed using IR spectroscopy (see spectra in the ESI). The IR spectrum of an equimolar mixture of $(Boc)_2O$ and $Br_3CCOCBr_3$ revealed the frequency assigned to the C=O stretching vibration at 1809 cm^{-1}, while the C=O stretching frequency of free $(Boc)_2O$ was present at 1812 and 1770 cm^{-1}. A similar result was also observed from the IR spectrum of the mixture of $(Boc)_2O$ and NBS, showing the frequencies of the C=O stretching vibration at 1809 and 1755 cm^{-1}. The shift of C=O stretching frequencies is probably caused by the coordination of $(Boc)_2O$ with $Br_3CCOCBr_3$ (or NBS), resulting in the disappearance of the β-dicarbonyl moiety of $(Boc)_2O$ in **TS-1** (Scheme 1).[16,38] A proposed mechanism is depicted in Scheme 1. Similar to the mechanism of the iodine-catalyzed reactions,[16] a carbonyl carbon of $(Boc)_2O$ is initially activated by donation of an oxygen lone pair to a partially positively charged bromine atom of $Br_3CCOCBr_3$ (or NBS) to generate **TS-1**. Then, nucleophilic attack by the amine on the electrophilic carbonyl carbon of **TS-1** produces **TS-2**, which decomposes to give the desired *N*-Boc-protected amine together with the formation of *tert*-butanol and carbon dioxide as by-products.

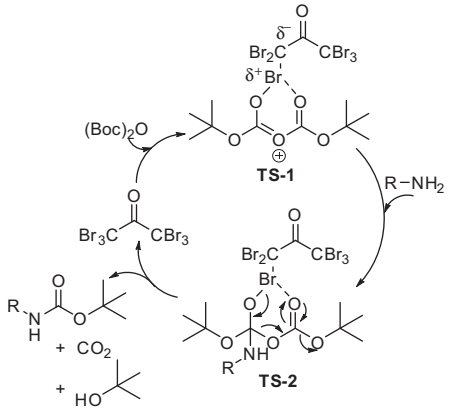

Scheme 1. Proposed mechanism.

In conclusion, we have described a mild and facile methodology for the *N*-*tert*-butyloxycarbonylation of amines utilizing NBS and $Br_3CCOCBr_3$ as catalysts. Aliphatic and aromatic amines could be chemoselectively converted to *N*-Boc protected products in good to excellent yields with short reaction times at room temperature.

Acknowledgements

This work was supported by the Thailand Research Fund for a New Researcher Grant (TRG5780085) and Faculty of Science, King Mongkut's University of Technology Thonburi (Grant No. SCI57-006). O. C. gratefully acknowledges Prof. Emmanuel A. Theodorakis,

Department of Chemistry & Biochemistry, University of California, San Diego for his valuable advice.

Supplementary data

Supplementary data (general procedure, spectral data and physical properties for all N-Bocprotected products, copies of IR spectra for the mechanistic study and copies of ^{1}H and ^{13}C NMR spectra for selected *N*-Boc protected products) associated with this article can be found, in the online version, at http://dx.doi.org/10.1016/j.tetlet.2016.09.052.

References and notes

1. Greene, T. W.; Wuts, P. G. M. In *Protecting Group in Organic Synthesis*; John Wiley and Sons: New York, 1999.
2. Pope, B. M.; Yamamoto, Y.; Tarbell, D. S. *Org. Synth. Coll.* **1988**, *VI*, 418.
3. Basel, Y.; Hassner, A. *J. Org. Chem.* **2000**, *65*, 6368.
4. Swenson, R. E.; Sowin, T. J.; Zhang, H. Q. *J. Org. Chem.* **2002**, *67*, 9182.
5. Harris, R. B.; Wilson, I. B. *Tetrahedron Lett.* **1983**, *24*, 231.
6. Kelly, T. A.; McNeil, D. W. *Tetrahedron Lett.* **1994**, *35*, 9003.
7. Sharma, G. V. M.; Janardhan Reddy, J.; Sree Lakshmi, P.; Radha Krishna, P. *Tetrahedron Lett.* **2004**, *45*, 6963.
8. Bartoli, G. B. M.; Locatelli, M.; Marcantoni, E.; Massaccesi, M.; Melchiorre, P.; Sambri, L. *Synlett* **2004**, 1794.
9. Heydari, A.; Hosseini, S. E. *Adv. Synth. Catal.* **2005**, *347*, 1929.
10. Rajanna, K. C. *Synth. Commun.* **2011**, *41*, 715.
11. Chankeshwara, S. V.; Chakraborti, A. K. *Tetrahedron Lett.* **2006**, *47*, 1087.
12. Suryakiran, N.; Prabhakar, P.; Reddy, T. S.; Rajesh, K.; Venkateswarlu, Y. *Tetrahedron Lett.* **2006**, *47*, 8039.
13. Suryakiran, N.; Prabhakar, P.; Reddy, T. S.; Srinivasulu, M.; Swamy, N. R.; Venkateswarlu, Y. *J. Mol. Catal. A: Chem.* **2007**, *264*, 40.
14. Chankeshwara, S. V.; Chakraborti, A. K. *Synthesis* **2006**, 2784.
15. Inahashi, N.; Matsumiya, A.; Sato, T. *Synlett* **2008**, 294.
16. Varala, R.; Nuvula, S.; Adapa, S. R. *J. Org. Chem.* **2006**, *71*, 8283.
17. Shailaja, M.; Manjula, A.; Rao, B. V. *Synth. Commun.* **2011**, *41*, 2073.
18. Heydari, A.; Khaksar, S.; Tajbakhsh, M. *Synthesis* **2008**, 3126.
19. Khaksar, S.; Heydari, A.; Tajbakhsh, M.; Vahdat, S. M. *Tetrahedron Lett.* **2008**, *49*, 3527.
20. Khaksar, S.; Vahdat, S. M.; Tajbakhsh, M.; Jahani, F.; Heydari, A. *Tetrahedron Lett.* **2010**, *51*, 6388.
21. Jahani, F.; Tajbakhsh, M.; Golchoubian, H.; Khaksar, S. *Tetrahedron Lett.* **2011**, *52*, 1260.
22. Upadhyaya, D. J.; Barge, A.; Stefania, R.; Cravotto, G. *Tetrahedron Lett.* **2007**, *48*, 8318.
23. Shirini, F.; Zolfigol, M. A.; Abedini, M. *J. Iran Chem. Soc.* **2010**, *7*, 603.
24. Shirini, F.; Khaligh, N. G. *Monatsh. Chem.* **2012**, *143*, 631.
25. Heydari, A.; Shiroodi, R. K.; Hamadi, H.; Esfandyari, M.; Pourayoubi, M. *Tetrahedron Lett.* **2007**, *48*, 5865.
26. Chankeshwara, S. V.; Chakraborti, A. K. *J. Mol. Catal. A: Chem.* **2006**, *253*, 198.
27. Kumar, K. S.; Iqbal, J.; Pal, M. *Tetrahedron Lett.* **2009**, *50*, 6244.
28. Das, B.; Venkateswarlu, K.; Krishnaiah, M.; Holla, H. *Tetrahedron Lett.* **2006**, *47*, 7551.
29. Atghia, S. V.; Sarvi Beigbaghlou, S. *J. Organomet. Chem.* **2013**, *745–746*, 42.
30. Shirini, F.; Mamaghani, M.; Atghia, S. V. *Catal. Commun.* **2011**, *12*, 1088.
31. Veisi, H.; Sedrpoushan, A.; Ghazizadeh, H.; Hemmati, S. *Res. Chem. Intermed.* **2016**, *42*, 1451.
32. Karmakar, B.; Banerji, J. *Tetrahedron Lett.* **2010**, *51*, 3855.
33. Chakraborti, A. K.; Chankeshwara, S. V. *Org. Biomol. Chem.* **2006**, *4*, 2769.
34. Khaligh, N. G.; Hazarkhani, H. *Monatsh. Chem.* **2014**, *145*, 1975.
35. Shirini, F.; Atghia, S. V.; Jirdehi, M. G. *Chin. Chem. Lett.* **2013**, *24*, 34.
36. Zolfigol, M. A.; Moosavi-Zare, A. R.; Moosavi, P.; Khakyzadeh, V.; Zare, A. *C. R. Chim* **2013**, *16*, 962.
37. Chaskar, A.; Yewale, S.; Langi, B.; Deokar, H. *J. Korean Chem. Soc.* **2009**, *53*, 422.
38. Sunitha, S.; Kanjilal, S.; Reddy, P. S.; Prasad, R. B. N. *Tetrahedron Lett.* **2008**, *49*, 2527.
39. Akbari, J.; Heydari, A.; Ma'mani, L.; Hosseini, S. H. *C. R. Chim.* **2010**, *13*, 544.
40. Karimian, S.; Tajik, H. *Chin. Chem. Lett.* **2014**, *25*, 218.
41. Shirini, F.; Jolodar, O. G.; Seddighi, M.; Borujeni, H. T. *RSC Adv.* **2015**, *5*, 19790.
42. Sarkar, A.; Roy, S. R.; Parikh, N.; Chakraborti, A. K. *J. Org. Chem.* **2011**, *76*, 7132.
43. Shirini, F.; Khaligh, N. G. *J. Mol. Liq.* **2013**, *177*, 386.
44. Majumdar, S.; De, J.; Chakraborty, A.; Maiti, D. K. *RSC Adv.* **2014**, *4*, 24544.
45. Reddy, M. S.; Narender, M.; Nageswar, Y. V. D.; Rao, K. R. *Synlett* **2006**, 1110.
46. Chankeshwara, S. V.; Chakraborti, A. K. *Org. Lett.* **2006**, *8*, 3259.
47. Vilaivan, T. *Tetrahedron Lett.* **2006**, *47*, 6739.
48. Siddaiah, V.; Basha, G. M.; Rao, G. P.; Prasad, U. V.; Rao, R. S. *Chem. Lett.* **2010**, *39*, 1127.
49. Zeng, H.; Li, Y.; Shao, H. *Synth. Commun.* **2012**, *42*, 25.
50. Jia, X.; Huang, Q.; Li, J.; Li, S.; Yang, Q. *Synlett* **2007**, 0806.
51. Dighe, S. N.; Jadhav, H. R. *Tetrahedron Lett.* **2012**, *53*, 5803.
52. Nardi, M.; Cano, N. H.; Costanzo, P.; Oliverio, M.; Sindona, G.; Procopio, A. *RSC Adv.* **2015**, *5*, 18751.
53. Tongkate, P.; Pluempanupat, W.; Chavasiri, W. *Tetrahedron Lett.* **2008**, *49*, 1146.
54. Menezes, F. G.; Kolling, R.; Bortoluzzi, A. J.; Gallardo, H.; Zucco, C. *Tetrahedron Lett.* **2009**, *50*, 2559.
55. Keller, L.; Beaumont, S.; Liu, J.-M.; Thoret, S.; Bignon, J. S.; Wdzieczak-Bakala, J.; Dauban, P.; Dodd, R. H. *J. Med. Chem.* **2008**, *51*, 3414.
56. Saito, Y.; Ouchi, H.; Takahata, H. *Tetrahedron* **2006**, *62*, 11599.

AAC Accepted Manuscript Posted Online 31 October 2016
Antimicrob. Agents Chemother. doi:10.1128/AAC.01220-16

Caged *Garcinia* xanthones: a novel chemical scaffold with potent antimalarial activity

Hangjun Ke,[a,#] Joanne M. Morrisey,[a] Shiwei Qu,[b] Oraphin Chantarasriwong,[c] Michael W. Mather, [a] Emmanuel A. Theodorakis,[b] Akhil B. Vaidya[a]

Center for Molecular Parasitology, Department of Microbiology and Immunology, Drexel University College of Medicine, Philadelphia, Pennsylvania, USA[a];

Department of Chemistry and Biochemistry, University of California, San Diego, La Jolla, California, USA[b];

Department of Chemistry, Faculty of Science, King Mongkut's University of Technology Thonburi, Bangmod, Thungkru, Bangkok, Thailand[c]

Running Head: Caged *Garcinia* Xanthones as novel antimalarial agents

[#] Address correspondence to Hangjun Ke, hangjun.ke@drexelmed.edu

Abstract

Caged *Garcinia* xanthones (CGXs) constitute a family of natural products that are produced by tropical/sub-tropical trees of the genus *Garcinia*. CGXs have a unique chemical architecture, defined by the presence of a caged scaffold at the C ring of a xanthone moiety and exhibit a broad range of biological activities. Here we show that synthetic CGXs exhibit antimalarial activity against *Plasmodium falciparum*, the causative parasite of human malaria, at the intra-erythrocytic stages. The activity can be substantially improved by attaching a triphenylphosphonium group at the A ring of the caged xanthone. Specifically, **CR135** and **CR142** were found to be highly effective antimalarial inhibitors with EC_{50}s (effective concentration that inhibits growth by 50%) as low as ~10 nM. CGXs affect malaria parasites at multiple intra-erythrocytic stages, with mature stages (trophozoites and schizonts) being more vulnerable than immature rings. Within hours of CGX treatment, malaria parasites display distinct morphological changes, significant reduction of parasitemia (the percentage of infected red blood cells) and aberrant mitochondrial fragmentation. CGXs, however, do not target the mitochondrial electron transport chain (mtETC), the target of the drug atovaquone and several preclinical candidates. The cytotoxicity of CGXs in human HEK293 cells is at the low μM level, which results in a therapeutic window around 150 fold for the lead compounds. In summary, we show that CGXs are potent antimalarial compounds with structures distinct from previously reported antimalarial inhibitors. Our results highlight the potential to further develop *Garcinia* natural product derivatives as novel antimalarial agents.

Introduction

Malaria remains a leading infectious disease in the tropical and subtropical regions of the world. In the past 15 years, the morbidity and mortality of malaria has decreased dramatically due to the wide use of artemisinin-combined chemotherapy (ACT), indoor residual spraying, the distribution of insecticide-treated bed nets, and other malaria prevention and research efforts (1-3). However, malaria parasites have evolved mechanisms to adapt to various immunological and chemical pressures. They display genomic plasticity, readily accumulating mutations and rearrangements to overcome antimalarial drugs (4). Clinical isolates that are resistant to the majority of antimalarial drugs available have spread widely in malaria endemic areas (5,6). The facile development and spread of parasite drug resistance clearly threatens the achievements made so far, as well as impeding the goal of eradicating malaria in the near future. The recent appearance and spread of artemisinin tolerance underscores the need for continued urgent efforts to develop new antimalarial reagents (7-9).

Plants of the genus *Garcinia* produce an intriguing family of caged xanthone-derived natural products that have a documented value in traditional Eastern medicine (10). Collectively referred to as caged *Garcinia* xanthones (CGXs), these compounds are structurally defined by an unusual motif in which the C-ring of an allylated xanthone has been converted into a tricyclic cage (Figure 1). This motif is further decorated via A-ring substitutions and peripheral oxidations to produce a variety of natural products with a broad range of bioactivities (11,12). Gambogic acid (**GBA**), the archetype of this family, potently inhibits cancer cell proliferation in solid tumors (13-17) and hematological malignancies (18), and has entered clinical trials in China for patients with non-small cell lung, colon and renal cancers (19). In addition, the ability of several CGXs to exhibit potent cytotoxicity at low μM concentrations has been well documented (20-23). Efforts to unveil the minimum structural motif of CGXs that is accountable for the observed anti-cancer activity led to the identification of cluvenone (**CLV**) (24,25). This compound was found to have

similar potency to **GBA** in inhibiting cancer cell growth against the NCI60 cell panel and a promising window of selectivity against non-tumor cells (26). Although the detailed mechanism of action of **GBA**, **CLV** and related compounds has not yet been delineated, several studies indicate that they localize to mitochondria and exhibit their bioactivity by affecting mitochondrial structure and function (27,28). Along these lines, the hydroxylated cluvenones **MAD28** and **MAD44** were recently found to bind to the mitoNEET family of iron-sulfur containing proteins that are located at the outer mitochondrial membrane (29).

The mitochondrion of malaria parasites is an essential organelle and has been validated as an antimalarial drug target (30,31). Compounds that disrupt essential mitochondrial functions within the parasite are either in clinical use or in clinical trials as potential antimalarial agents (32) . For instance, atovaquone (a component of Malarone®) is a clinically approved drug that selectively inhibits the parasite mitochondrial electron transport chain (mtETC) at the cytochrome bc_1 complex, leading to collapse of the mitochondrial membrane potential (33). Moreover, the dihydroorotate dehydrogenase (DHODH) inhibitor DSM265 is currently undergoing Phase II clinical trials (34). Inhibition of DHODH blocks pyrimidine biosynthesis, which is an essential pathway in malaria parasites (35). Since malaria parasites require mitochondrial functions for survival, we speculated that **GBA** and derivative compounds might exhibit antimalarial activity. In this study, we examine the antimalarial activities of **GBA** and synthetic CGXs against the human malaria parasite *Plasmodium falciparum*.

Materials and Methods

1. Parasite lines and parasite culture. *P. falciparum* strains Dd2 (resistant to chloroquine, mefloquine and pyrimethamine) and 3D7 (drug sensitive) are the wild type lines used in this study. *P. falciparum* 3D7attB-yDHODH is a transgenic line bearing a copy of the yeast dihydroorotate dehydrogenase gene (yDHODH) in the genome, rendering the parasites

resistant to inhibitors targeting the mitochondrial electron transport chain (mtETC) (35,36). Parasites were cultured in human O^+ erythrocytes (Interstate Blood Bank) in complete RPMI 1640 medium supplemented with 0.5% AlbuMAX (Invitrogen), 15 mM HEPES, 10 mg/L hypoxanthine, 25 mM $NaHCO_3$ and 50 µg/L gentamicin. Cultures were incubated at 37 °C in an incubator filled with a low oxygen gas mixture (89% N_2, 5% CO_2, and 6% O_2).

2. Growth inhibition assay via ^{3}H-hypoxanthine incorporation. The antimalarial activity was determined by measuring ^{3}H-hypoxanthine incorporation in parasites exposed to compounds in 96-well plates. Compounds tested were initially dissolved in DMSO at 10 mM concentrations. Parasite cultures at 1% parasitemia and 1.5% hematocrit were exposed to serial dilutions of each compound or no compound media for 24 h. After 24 h, each well was pulsed with 0.5 µCi of ^{3}H-hypoxanthine and incubated for another 24 h. Then parasites were frozen at -80 °C overnight. Parasites were lysed by thawing and nucleic acids were collected onto filters using a cell harvester (PerkinElmer Life Sciences). Filters were dried by air, and 30 µl MicroScint O (PerkinElmer Life Sciences) was added to each well. Incorporation of ^{3}H-hypoxanthine was quantified by a TopCount scintillation counter (PerkinElmer Life Sciences).

3. Flow cytometry assessment of parasitemia. Dd2 parasites were tightly synchronized by multiple rounds of alanine treatment (0.5 M alanine/10 mM HEPES, pH 7.6) of ring stage cultures (37). Upon reaching the mid-trophozoite stage, synchronized parasites were inoculated into a 24-well plate with each well harboring a 2 ml culture with 2.5% hematocrit. Parasites were exposed to DMSO (0.5 µl/ml) or compounds at 10x EC_{50} concentration. Specifically, the concentrations were 0.1 µM, 0.15 µM, 2.6 µM and 1.1 µM for **CR135**, **CR142**, **MAD28**, **SQ129**, respectively. At specified time points post treatment (2 h, 4 h, 8 h, 24 h and 48 h), a small aliquot was taken from each well and used to prepare a Giemsa-stained thin smear for morphological examination. At the same time points, another aliquot of each parasite culture (5-

10 µl of pellet) was fixed with 4% formaldehyde at 37 °C for 1 h or 4 °C overnight on a rotator. The samples were then washed three times with PBS and stained with SYBR Green (ThermoFisher Scientific) for 1h at room temperature on a rotator. They were then washed three times and ~1 µl of the pellet was resuspended in 1 ml of sterile H_2O. The samples were analyzed by a BD Accuri C6 flow cytometer. Uninfected RBCs, unstained and stained with SYBR Green, and unstained infected trophozoites were used as controls. For each sample, 1,000,000 events were collected and cell debris was removed by proper gating strategy. The percentage of SYBR Green positive events was taken to be the parasitemia.

4. Microscopy. Thin blood smears were fixed with 100% methanol, air dried and stained with Giemsa dye solution for 10 min. Morphologies of infected red blood cells were examined under a Leica microscope and pictures were taken with a 16-megapixel camera. When parasitemia was determined microscopically, at least 1000 red blood cells were counted. For mitochondrial morphologies, parasites were stained with MitoTracker Red (Invitrogen) at 60 nM for 30 min, washed three times with PBS, and then incubated with a test compound. After compound treatment, parasites were lightly fixed with 1% formaldehyde for 10 min and observed under an Olympus fluorescence microscope.

5. Immunofluorescence Assay (IFA). Dd2 parasites were tightly synchronized with several rounds of alanine treatment. At the early trophozoite stage, parasites were exposed to DMSO or a 10xEC_{50} concentration of selected CGX compounds for 8 h. 30 min before sample harvesting, 60 nM MitoTracker Red CMXRos (Invitrogen) was added to each culture. Parasites were then washed 3 times with PBS. Thin blood smears were made for each condition. The remaining cultures were fixed with 4% formaldehyde/0.0075% glutaraldehyde at 4 °C overnight. The samples were then permeabilized with 0.1%Triton X-100, reduced with 0.1 mg/ml sodium borohydride, and blocked with 5% BSA-PBS, according to our standard IFA procedure (38). To

monitor the morphological changes of the food vacuole upon drug treatment, an anti Plasmepsin II polyclonal antibody (Rabbit antiserum MRA-66) was obtained from BEI Resources (NIAID and NIH) (BEIResources.org). The antibody was diluted 1:1000 and incubated with the samples at 4 °C overnight. Then an AlexaFluor 488 conjugated anti-rabbit secondary antibody (Molecular Probes) was added at a dilution of 1:350 and incubated at 4 °C overnight. All other steps followed the standard protocol (38). The parasites were then visualized under the Olympus fluorescence microscope.

6. MTT cell growth assay. HEK293 is a non-carcinoma cell line stably transformed with adenovirus DNA and can grow indefinitely *in vitro* (39). The mammalian cells were cultured with complete Dulbecco's Modified Eagle's Medium (DMEM) supplemented with 10% fetal bovine serum. The cytotoxicity of CGX compounds against HEK293 cells was determined by an MTT (3-(4,5-dimethylthiazol-2-yl)-2,5-diphenyltetrazolium bromide) assay in 96 well plates following the manufacture's protocol (EMD Millipore Corporation). Briefly, 10, 000 cells in a volume of 50 µl DMEM were inoculated into each well. The plates were incubated in a 37 °C incubator (5% CO_2) for 2 h to allow the cells to attach. Compounds were then serially diluted in another 96 well plate and 50 µl aliquots with various concentrations were added into wells previously seeded with cells. The final volume of medium in each well equaled 0.1 ml. After exposure to compounds for 24 h and 48 h, 10 µl of MTT solution (5 mg/ml) was added to each well and the plates were incubated at 37 °C for 4 h to allow MTT to be reduced to purple formazan in live cells. At the end of 4 h incubation with MTT, 100 µl isopropanol containing 0.04 N HCl was added to each well. The isopropanol dissolves formazan, yielding homogenous blue solution that can be measured colorimetrically. Absorbance was measured with an ELISA plate reader (Tecan US) at 570 nm versus a reference wavelength of 630 nm.

7. Compound synthesis. **GBA** was isolated from gamboge resin via its pyridine salt (27). **CLV** and the hydroxylated cluvenones **MAD28** and **MAD44** were synthesized as previously reported (25,40). The synthesis of the triphenylphosphonium salt conjugates is shown in Supplementary Material. **CR135** and **CR142** were synthesized from **MAD28** and **MAD44**, respectively, by treating them with 1,4-dibromobutane (5 equiv) and potassium carbonate (2 equiv) in dimethylformamide (DMF) (41). The resulting bromide was then converted to the triphenylphosphonium salt upon treatment with Ph_3P (5 equiv) in acetonitrile at 150 °C under microwave irradiation. Preparation of **SQ129** proceeded in three steps that included: (a) protection of the catechol functionality of trihydroxylated xanthone (42,43) with diiodomethane and sodium bicarbonate; (b) bromination of the C_6 phenol with 1,4-dibromobutane and (c) treatment of the resulting bromide with triphenylphosphine. Detailed experimental procedures and spectroscopic and analytical data are shown in the Supplemental Material.

8. Data analysis. For ^{3}H-hypoxanthine incorporation and MTT assays, triplicate wells were set for each condition tested. The mean values of measurements made with parasites or HEK293 cells treated with DMSO alone were set as 100%. All other measurements were compared to DMSO controls. The dose-response data was then analyzed by GraphPad Prism Version 4 to obtain curves fitted by nonlinear regression and corresponding EC_{50} values. The mean±standard error of all biological replicates for each condition is reported in the Results.

Results

Effect of CGXs on the growth of the human malaria parasite *P. falciparum*. The erythrocytic stage of malaria parasites causes all clinical symptoms associated with malaria and is the target for most antimalarial drugs. *P. falciparum* strains isolated from various geographical regions harbor different sensitivities to antimalarial drugs. Dd2 is a multi-drug resistant clone selected from an Indochina isolate using mefloquine pressure (44). To test if **GBA** and related

CGXs (Figure 1) have activities against drug resistant parasites, we performed growth inhibition assays based on ^{3}H-hypoxanthine incorporation by Dd2 parasites (Figure 2). Artemisinin was included as a control in this assay, which yielded an EC_{50} value of 12.4±1.5 nM, similar to previous reports (45). As shown in Figure 2, **GBA** and **CLV** exhibited moderate antimalarial activities with EC_{50} values of 0.28±0.03 μM and 0.75±0.03 μM, respectively. A similar antimalarial activity was observed with **MAD28**, the C_6 hydroxylated **CLV**, which exhibited an EC_{50} of 0.26±0.02 μM. However, **MAD44**, the C_{18} hydroxylated **CLV**, was less effective, with an EC_{50} of 4.1±0.3 μM. **CR135** and **CR142** were synthesized from **MAD28** and **MAD44**, respectively, by conjugating a triphenylphosphonium group at C_6 of **MAD28** and C_{18} of **MAD44** (41). Importantly, **CR135** and **CR142** exhibited remarkable antimalarial activities, with EC_{50}s as low as 7.9 nM and 11.1 nM, respectively. Thus, conjugating the A ring of the caged xanthone structure with a triphenylphosphonium group drastically improves the antimalarial activity. Specifically, adding this group to the C_6-hydroxyl group of **MAD28** decreased the EC_{50} by about 30 fold from 267 nM (**MAD28**) to 7.9 nM (**CR135**). The same modification at the C_{18}-hydroxyl group decreased the EC_{50} about 370 fold from 4100 nM (**MAD44**) to 11.1 nM (**CR142**). To test if a caged xanthone was required for the robust activity of **CR135**, we replaced the caged xanthone structure of **CR135** with a planar xanthone, yielding the compound **SQ129**. The antimalarial activity of **SQ129** (EC_{50}, 106.5±13.1 nM) was much weaker than that of **CR135** (Figure 2), suggesting that a caged xanthone moiety is also needed for optimal antimalarial activity.

We repeated the growth inhibition assays several times with selected CGX compounds in drug sensitive (3D7) and drug resistant (Dd2) *P. falciparum* parasites and the average EC_{50} values are presented in Table 1. Collectively, these data show that **GBA** and related CGXs have moderate antimalarial potency, but their efficacy increases dramatically upon conjugation of the caged xanthone motif with a triphenylphosphonium group.

Effect of CGXs on the intra-erythrocytic development cycle of *P. falciparum*. Within the red blood cells, *P. falciparum* undergoes a 48 h intra-erythrocytic development cycle, during which the maturation process can be subdivided into ring, trophozoite, and schizont stages (46). Compounds **CR135**, **CR142** and **MAD28,** which exhibited the best EC_{50} values, were selected for this study while DMSO and **SQ129** served as controls. We tightly synchronized Dd2 parasites and subsequently treated them at the trophozoite stage with CGX compounds at 10x EC_{50} concentrations (Materials and Methods) and monitored them from 2 h to 48 h post addition. At each time point, thin blood smears were prepared for morphological studies, and parasite aliquots were fixed and stained with SYBR Green for determination of parasitemia by flow cytometry.

Parasite morphological changes and parasitemia during the treatment time course are presented in Figure 3. In the DMSO control, parasites progressed normally throughout the 48 h life cycle (Figure 3A, top panel). However, trophozoites treated with **CR135** or **CR142** displayed a characteristic morphological change, the appearance of a large Giemsa stain resistant area (Figure 3A, red arrows), giving the appearance of an empty volume that fills much of the parasite, as soon as 2 h after treatment. For future references, we named this morphologically aberrant structure as Giemsa-stain negative body (GNB). The proportion of these GNB parasites containing a large stain-negative structure increased from ~20% (2 h drug treatment) to ~30% after 4 h drug treatment (Figure 3B). In samples treated with **CR135** or **CR142** for 8 h, the proportion of empty-looking parasites decreased to ~ 5%, due to the progression of the parasite growth cycle producing a large population of newly invaded erythrocytes containing young ring parasites (Figure 3B). These newly formed ring stage parasites seemed to be morphologically normal (Figure 3A). During an additional 16 h exposure to **CR135** or **CR142** (24 h total), these new rings progressed to late rings without any observable morphological defects (Figure 3A). However, in the next 24 h (48 h total post addition, Figure 3A), growth

appeared to become blocked at the early trophozoite stage, with the blocked parasites regaining the characteristic empty-looking appearance.

On the other hand, **MAD28** seemed to kill parasites by different mechanism(s). As shown in Figure 3A, **MAD28** did not cause the formation of a large empty area inside parasites during the treatment time course. Nevertheless, at the concentration tested (2.6 μM), **MAD28** significantly delayed progression of the parasites. After 4 h treatment, fewer trophozoites progressed to multi-nucleated schizonts. After 8 h **MAD28** treatment, there were very few new rings in the sample. **SQ129** behaved distinctly from **CR135**/**CR142** or **MAD28** (Figure 3A). It did not induce a large GNB in the parasites or inhibit parasite growth as dramatically as **MAD28**. In all, these data suggest that **CR135** works similarly to **CR142**; however, **CR135** and **CR142** kill malaria parasites through mechanism(s) distinct from those of **MAD28**.

Quantitative parasitemia data for the same 48 h treatment time course, determined by flow cytometry, is presented in Figure 3C. **CR135** and **CR142** knocked down parasitemia significantly after drug treatment for 24 h. Even though there were some residual “parasites” present after drug treatment for 48 h with **CR135** or **CR142**, these parasites were dead and did not progress (Figure 3A). After a 96 h treatment with **CR135** or **CR142**, the parasitemia dropped down to an undetectable level, and there were just a few dead remnant parasites or purple dots within the host cells observed after staining (data not shown). **MAD28**, on the other hand, seemed to be a faster killer than **CR135** or **CR142**. It reduced the parasitemia significantly after 8 h of drug treatment (Figure 3B). The kinetics of these parasite killing data suggests that **CR135** and **CR142** eliminate parasites at a slower pace than does **MAD28** and, again, it appears that **CR135** and **CR142** work similarly, while **MAD28** kills parasites through different mechanism(s).

As shown in Figure 3A, CR135 and CR142 caused the formation of a large Giemsa stain resistant area (GNB) inside the parasite. It was noticeable that this large empty area was adjacent to the hemozoin crystal. The intimate localization of this structure to hemozoin prompted us to investigate the integrity of the food vacuole under drug treatment with CR135 and CR142 by IFA using a food vacuole marker. Dd2 parasites were synchoronized and treated with CR135 and CR142 (10x EC_{50} concentration), respectively, for 8 h from early-trophozoite stage to mid-trophozoite stage. Compared to a 4 h treatment starting with mid trophozoites, we noticed that the percentage of GNB parasites increased significantly (up to 50%) when treatment started at a younger trophozoite stage and lasted longer (8 h) (data not shown). Post treatment, the parasites were then fixed with formaldehyde/glutaraldehyde. An anti Plasmepsin II polyclonal antibody was used to visualize the structure of food vacuole; Plasmepsin II, an aspartic protease for hemoglobin digestion, is a marker for this organelle (47,48). As shown in Figure 4, in the control parasite, one, relatively large globular structure containing the hemozoin crystal was clearly visible, and a few small spots next to the main body were also present. This staining pattern represents the normal food vacuole architecture (47,48). Under treatment with CR135 and CR142, however, the intactness of the food vacuole appeared to be lost. As shown in Figure 4, the main globular staining disappeared; instead, there were many small granular fluorescing particles scattering throughout the cytosol, suggesting that the food vacuole integrity was damaged by treatment with the compounds. A correlation between the large vacant space in the GNB parasites (Figure 3A) and the IFA images (Figure 4) is not evident; thus, the nature of this feature remains unclear at present (see Discussion).

To further characterize the effects of these CGX compounds on parasites, we also treated *P. falciparum* with 10x EC_{50} concentrations starting with synchronized schizonts and with synchronized rings. As shown in the Supplementary Figure 1A, when treatment was begun at the schizont stage, these compounds significantly inhibited parasite development. At 10x EC_{50}

concentration, **MAD28** was the most effective compound in this regard. As shown in Supplementary Figure 1B, when a parasite culture at 5% schizont parasitemia was treated with **MAD28**, the parasitemia only declined to 3% after 8 h treatment, indicating that ~60% of the schizonts still remained inside the host cells. In control parasites treated with DMSO in parallel, only ~10% of the schizonts had not egressed after 8 h incubation. **CR135** and **CR142** also inhibited parasite growth, but to a lesser extent than **MAD28**. Due to the strong inhibitory effect of **MAD28**, the parasitemia after 24 h treatment dropped to a very low level (Supplementary Figure 1C). Again, **CR135** and **CR142** were slow killers, and parasitemias after 24 h drug treatment remained much higher than that of **MAD28** (Supplementary Figure 1C). Collectively, these data suggest that CGX compounds inhibit parasite growth at the schizont stage, possibly via blocking schizont maturation and/or parasite egress. MAD28 was a strong inhibitor at the concentration used (2.6 μM). However, due to its narrow therapeutic window, MAD28 is quite toxic to mammalian cells at 10x EC_{50} concentration (see Table 1).

Different phenomena were observed when treatments were initiated at the ring stage. As shown in Supplementary Figure 2A, the compounds did not inhibit the progression of young rings to mature rings significantly, as 8 h drug treatments did not cause dramatic morphological changes. For all the compounds tested, the parasitemia of an 8 h drug treatment was comparable to that of the control DMSO treatment (Supplementary Figure 2B). The antimalarial effects of these compounds became much more evident after 24 h of drug treatment: **CR135** and **CR142** arrested the parasites at early trophozoite stages and formed a large GNB inside the parasites; **MAD28** blocked the parasites at an earlier stage, but did not cause the formation of a large empty-looking structure. The parasitemias after 24 h of treatment with each of the compounds are presented in Supplementary Figure 2C.

Mitochondrial morphology of *P. falciparum* parasites treated with CGXs. GBA and CGXs are pleiotropic compounds that kill cancer cells via multiple mechanisms (11). One important target is the mitochondrion, which undergoes apoptosis under drug treatment (27). **MAD28** has been recently shown to inhibit an iron-sulfur cluster binding protein, mitoNEET, on the outer membrane of mitochondria in breast cancer cells (29). MitoNEET is involved in cellular iron homeostasis and various mitochondrial functions (49).

To determine the effects of these compounds on parasite mitochondria, we preloaded synchronized parasites at the early trophozoite stage with MitoTracker (Materials and Methods), treated them with compounds at 10x EC_{50} concentrations, and observed their mitochondrial morphologies over time. In parasites treated with **CR135**, **CR142**, or **MAD28** for 4 h, their mitochondria were morphologically indistinguishable from those treated with DMSO vehicle (data not shown). However, in samples treated with compounds for 8 h, we observed significant morphological changes in the mitochondria (Figure 5). As shown in Figure 5A, in the DMSO control parasite, the mitochondrion formed a continuous tubular filament structure, indicating a healthy mitochondrion. However, in parasites treated with **CR135**, **CR142**, or **MAD28**, the mitochondria appeared fragmented and punctate. Each parasite contained one or several MitoTracker stained dots, but no long tubular structures. To further quantify this phenomenon, we examined 200 parasites from each treatment (drug or vehicle) and classified them as having either tubular mitochondria or punctate mitochondria. As shown in Figure 5B, in the DMSO control, >95% of the parasites had tubular structures; however, the percentage of tubular mitochondria decreased to <5% in drug treated parasites. These data strongly suggest that these CGX compounds have a strong detrimental effect on the parasite mitochondria.

Effect of CGXs on the mitochondrial electron transport chain (mtETC). During the asexual blood stages, the mtETC of malaria parasites is required to recycle ubiquinol to ubiquinone,

which serves as the electron acceptor for DHODH, an essential enzyme in the pyrimidine biosynthesis pathway (35). Providing the parasite with a yeast DHODH enzyme that utilizes a different electron acceptor establishes an alternate pathway for pyrimidine biosynthesis and renders the parasite resistant to all bc_1 complex inhibitors (35). Thus, yDHODH transgenic lines have become a convenient tool to determine if a compound targets the mtETC. Here, we utilized the 3D7attB-yDHODH line, which has the yDHODH gene integrated into the genome at a non-essential locus (36). As shown in Figure 6, this transgenic line was fully resistant to atovaquone, as expected, but was still susceptible to all CGX compounds tested, suggesting that the target(s) of the CGXs do not reside in the parasite mtETC. Consequently, these drugs likely target other essential function(s), either inside or outside of the mitochondrion. We note that the EC_{50} values of these compounds against the 3D7attB-yDHODH parasites (Figure 65) were slightly higher than those found with the 3D7 parasites (Table 1). The reasons for the variation are undetermined at present, but possibly may arise during the genetic transfections and lengthy selection procedures required to generate the 3D7attB-yDHODH line.

Toxicity of CGXs to human cells. To test the toxicity of these CGXs to human cells, we performed the standard MTT assay on HEK293 cells. The cells were exposed to a range of concentrations of each selected CGX compound for 24 h and 48 h, as described in Materials and Methods. As shown in Figure 7, after 24 h drug exposure, we found that the EC_{50}s of **CR135**, **CR142** and **MAD28** fell in the range of low μM concentrations. **SQ129** was less toxic to HEK293 cells with a significantly higher EC_{50}. The average EC_{50} values from 3 independent experiments are shown in Table 1. The EC_{50} values for the 48 h drug exposure were quite similar to those of the 24 h treatment (data not shown). These data suggest that these CGX compounds are toxic to human cells at low μM concentrations. Accordingly, the therapeutic window is around 150 fold for **CR135** or **CR142**, while it is much narrower for **MAD28** (~7 fold).

Discussion

In this study, we tested the antimalarial activities of CGX compounds against *P. falciparum* malaria parasites at the intra-erythrocytic stages. **GBA** and synthetic derivatives have been of great interest to medicinal chemistry due to their potent activities against cancer cells. For the first time, this study shows that these compounds also possess antimalarial activity both against drug sensitive and drug resistant parasite lines. Our data extend the biological functions of **GBA** and CGXs beyond their known anticancer (11), antibacterial (50), and antiviral (51) effects to include antiparasitic activity.

GBA and its derivatives showed moderate antimalarial activity with EC_{50}s at sub micromolar concentrations. This activity was greatly enhanced for compounds **CR135** or **CR142**, in which the caged xanthone motif was conjugated with a triphenylphosphonium group, resulting in EC_{50}s at low nM concentrations. It has been proposed that delocalized lipophilic cations, such as the triphenylphosphonium group, can specifically and efficiently drive their cargo to active mitochondria, which maintain a negative-inside transmembrane gradient (52,53). Such a delivery strategy has led to the development of MitoQ, a ubiquinone-triphenylphosphonium conjugate that has entered clinical trials against neurodegenerative diseases (54,55). Moreover, improvement of antimalarial potency has been reported for a series of 1,4-naphthoquinones (the chemical class that include atovaquone) conjugated with a triphenylphosphonium group (56,57). In the infected red blood cell, the parasite's mitochondrion is the organelle with the most negative membrane potential. Therefore, we reason that **CR135** and **CR142** accumulate in or at the parasite's mitochondrion in higher concentrations compared to the rest of the parasite and the host. In turn, the parasite mitochondrion is likely a major action site for these compounds. In support of this hypothesis, we also observed that **CR135** and **CR142** caused mitochondrial fragmentation in the parasite 8 h post drug treatment (Figure 4), indicating that the parasite mitochondrion contains, at least, one target of **CR135** and **CR142**. Interestingly, in cancer cells,

both **CR135** and **CR142** showed decreased toxicity compared to their parental compounds, **MAD28** and **MAD44** (41), suggesting that structural modifications of the CGX motif could improve both potency and selectivity against malaria parasites. Besides the triphenylphosphonium group, the caged xanthone moiety of **CR135** and **CR142** is also critical for function since **SQ129**, a synthetic derivative that contains a triphenylphosphonium group but lacks the caged xanthone, showed only moderate antimalarial activity.

We found that CGXs kill malaria parasites at multiple asexual stages. The metabolically active trophozoite and schizont stages are more sensitive to these compounds compared to the ring stage parasites (Figure 3). Our data also show that treatment with different CGXs caused distinct morphological changes to the parasites, suggesting that the various individual modifications to these compounds may result in differing modes of action. Particularly, **CR135** and **CR142** exhibited antimalarial activities at low nanomolar concentrations (Figure 2). These compounds caused the formation of a large Giemsa-stain negative structure (GNB) inside the parasite that occurred during trophozoite development (Figure 3). The appearance of GNB seemed to be specific for **CR135** or **CR142**, not for **MAD28** (Figure 3). Since this enlarged area was close to the hemozoin particle (Figure 3), we thought that it might be an enlargement of the food vacuole. Indeed, the integrity of food vacuole was damaged by **CR135** and **CR142** treatment as determined by IFA with a food vacuole marker (Figure 4). Under drug treatment (**CR135** or **CR142**), the globular structure of the food vacuole of a normal parasite was absent, and the vacuole marker Plasmepsin II distributed among many punctate particles scattered throughout the parasite cytosol (Figure 4). These small particles, however, did not appear to outline a large structure resembling the empty area seen in Giemsa stained parasites after drug treatment (compare Figure 3 and Figure 4). Therefore, at present, the nature of GNB seen in thin blood smears remains unknown.

441 At present, the mechanisms of action of CGXs against malaria parasites remain unknown. In
442 cancer cells, **GBA** and other CGXs are known to cause mitochondrial damage and apoptosis
443 (11). The mtETC is an essential process in malaria parasites and a known antimalarial drug
444 target. We have shown that in the asexual blood stages, the critical function of the mtETC is to
445 sustain the activity of the parasite dihydroorotate dehydrogenase (DHODH) for pyrimidine
446 biosynthesis (35,36). Provision of the parasites with the yeast DHODH, which does not rely on
447 the mtETC, makes the parasites resistant to all mtETC inhibitors (35,36). Importantly however,
448 yeast DHODH transgenic parasites were found to be sensitive to CGXs (Figure 5). This result
449 rules out the possibility that CGXs target the mtETC. It is likely that **CR135** and **CR142** target
450 other as yet unknown essential mitochondrial function(s) or other pathways beyond the
451 mitochondrion.
452
453 CGX compounds seem to target multiple pathways. The integrity of food vacuole is lost after 8 h
454 of treatment with **CR135** and **CR142**. We attempted to generate resistant clones by culturing
455 10^8 Dd2 parasites under 3x EC_{50} and 5x EC_{50} of **CR135**, **CR142**, and **MAD28**, individually.
456 However, none of these conditions yielded any resistant parasites over a two month period
457 (data not shown), consistent with the assumption that CGX compounds have various targets.
458 Targeting multiple pathways can be beneficial to prevent or delay the appearance of drug
459 resistance. Indeed, the standard antimalarial chemotherapy involves the use of several agents
460 in a combination, since monotherapy can often select resistant parasites rapidly. Therefore, it
461 could be an advantage for CGX compounds to target multiple pathways. On the other hand,
462 action against multiple targets can make it challenging to optimize parasite specific inhibitors via
463 a rational program of chemical modifications. CGX compounds kill mammalian cells at low
464 micromolar concentrations (1.5-2.2 μM; Figure 7), somewhat below the common concentration
465 (>10 μM) for other antimalarial compounds under development. While the initial GCX
466 compounds had a narrow selective window, addition of a triphenylphosphonium group to the

xanthone moiety expanded the therapeutic window dramatically from 7 fold (**MAD28**) to 150 fold (**CR135**/**CR142**) (Table 1). Thus, it is possible to develop better CGX derivatives through medicinal chemistry. As the most efficient antimalarial compound of the series, **CR135** could be a lead for future chemical optimization.

From a drug development point of view, **GBA** and related CGXs clearly have potential for further development as antimalarial drugs. Importantly, conjugation of the CGX motif with selective transporters and delivery systems can substantially improve the potency and target selectivity. This was shown by **CR135** and **CR142,** which exhibit strong antimalarial activity at low nanomolar concentrations. It is thus reasonable to predict that further chemical optimization of the caged xanthone backbone would yield compounds with more potent and selective antimalarial activities. Interestingly, CGX compounds were not included in the “malaria box”, a set of 400 antimalarial compounds made available to the research community by Medicines for Malaria Venture and partner companies and organizations (58). The CGX compounds appear to represent a new and unexplored class of antimalarial agents with a totally different chemical backbone from those of other chemical scaffolds discovered by high through-put screenings or other methods.

GBA and gamboge have been used in Eastern medicine for hundreds of years. **GBA** has entered a Phase II clinical trial in China as an anti-cancer agent in patients with non-small cell lung, colon and renal cancers (19).Toxicity studies on **GBA** in mice, dogs, and rats indicated that **GBA** has decent therapeutic windows for cancer therapies (59,60) without inducing any toxic symptoms on blood pressure, heart rate and respiratory frequency at pharmacologically relevant doses (61). An innocuous dose of GBA in rats was established to be 60 mg/kg after administration for a total of 13 weeks at a frequency of one administration every other day. This dose was more than 10 times higher than that used in human clinical trials (58, 59). In addition,

493 bioavailability studies (40 and 80 mg/Kg) in rats showed that GBA was rapidly accumulated in
494 liver where it can be metabolized by various routes, including oxidation, hydration,
495 glutathionylation and glucosidation, and was mainly excreted in bile from 0-24 h post-dosing
496 (62,63). These studies attest to the pharmacological potential of GBA and the CGX motif.
497 Moreover, the developed synthetic strategies allow rapid and high yielding access to designed
498 CGX analogs thereby potentially paving the way for the development of CGX-based antimalarial
499 agents.
500
501 In conclusion, we evaluated the effect of gambogic acid and related synthetic analogues of
502 caged *Garcinia* xanthones as antimalarial agents. We found that these compounds induce
503 cytotoxicity in *P. falciparum* malaria parasites at submicromolar concentrations. Importantly,
504 conjugating these compounds with a phosphonium salt improved the efficacy by about two
505 orders of magnitude, resulting in lead compounds with a promising therapeutic window. Further
506 modification of the caged xanthone motif and/or the delivery subunit could further increase the
507 selective cytotoxicity of the compound and lead to the development of a promising lead
508 candidate.
509
510 **Acknowledgement**
511 The Plasmepsin II antibody was obtained through BEI Resources (NIAID and NIH). The
512 antibody was originally contributed by Daniel E. Goldberg from Washington University at St.
513 Louis. We thank Dr. James M. Burns Jr. from Drexel University College of Medicine for help in
514 arranging the delivery of antibody. Human embryonic kidney cells (HEK293) were kindly
515 provided by Dr. Sandhya Kortagere from Drexel University College of Medicine. We thank Dr.
516 Wei Xu for technical assistance in culturing HEK293 cells and Sihem Sassi-Gaha for help with
517 MTT assays. We also thank Dr. Anthony Mrse (UCSD NMR Facility) and Dr. Yongxuan Su
518 (UCSD MS Facility) for assistance with the spectroscopic characterizations.

Funding information

This work was support by grants AI028398 from NIH to Dr. Akhil B. Vaidya, CRC-15-380737 from Cancer Research Coordinating Committee to Dr. Emmanuel A. Theodorakis, and TRG5780085 from Thailand Research Fund to Dr. Oraphin Chantarasriwong.

Reference

1. WHO (ed) (2015) *World Malaria Report*
2. Crompton, P. D., Moebius, J., Portugal, S., Waisberg, M., Hart, G., Garver, L. S., Miller, L. H., Barillas-Mury, C., and Pierce, S. K. (2014) Malaria immunity in man and mosquito: insights into unsolved mysteries of a deadly infectious disease. *Annu Rev Immunol* **32**, 157-187
3. White, N. J., Pukrittayakamee, S., Hien, T. T., Faiz, M. A., Mokuolu, O. A., and Dondorp, A. M. (2014) Malaria. *Lancet* **383**, 723-735
4. Miller, L. H., Ackerman, H. C., Su, X. Z., and Wellems, T. E. (2013) Malaria biology and disease pathogenesis: insights for new treatments. *Nat Med* **19**, 156-167
5. Cui, L., Mharakurwa, S., Ndiaye, D., Rathod, P. K., and Rosenthal, P. J. (2015) Antimalarial Drug Resistance: Literature Review and Activities and Findings of the ICEMR Network. *Am J Trop Med Hyg* **93**, 57-68
6. Takala-Harrison, S., and Laufer, M. K. (2015) Antimalarial drug resistance in Africa: key lessons for the future. *Ann N Y Acad Sci* **1342**, 62-67
7. Ashley, E. A., Dhorda, M., Fairhurst, R. M., Amaratunga, C., Lim, P., Suon, S., Sreng, S., Anderson, J. M., Mao, S., Sam, B., Sopha, C., Chuor, C. M., Nguon, C., Sovannaroth, S., Pukrittayakamee, S., Jittamala, P., Chotivanich, K., Chutasmit, K., Suchatsoonthorn, C., Runcharoen, R., Hien, T. T., Thuy-Nhien, N. T., Thanh, N. V., Phu, N. H., Htut, Y., Han, K. T., Aye, K. H., Mokuolu, O. A., Olaosebikan, R. R., Folaranmi, O. O., Mayxay, M., Khanthavong, M., Hongvanthong, B., Newton, P. N., Onyamboko, M. A., Fanello, C. I., Tshefu, A. K., Mishra, N., Valecha, N., Phyo, A. P., Nosten, F., Yi, P., Tripura, R., Borrmann, S., Bashraheil, M., Peshu, J., Faiz, M. A., Ghose, A., Hossain, M. A., Samad, R., Rahman, M. R., Hasan, M. M., Islam, A., Miotto, O., Amato, R., MacInnis, B., Stalker, J., Kwiatkowski, D. P., Bozdech, Z., Jeeyapant, A., Cheah, P. Y., Sakulthaew, T., Chalk, J., Intharabut, B., Silamut, K., Lee, S. J., Vihokhern, B., Kunasol, C., Imwong, M., Tarning, J., Taylor, W. J., Yeung, S., Woodrow, C. J., Flegg, J. A., Das, D., Smith, J., Venkatesan, M., Plowe, C. V., Stepniewska, K., Guerin, P. J., Dondorp, A. M., Day, N. P., White, N. J., and Tracking Resistance to Artemisinin, C. (2014) Spread of artemisinin resistance in Plasmodium falciparum malaria. *N Engl J Med* **371**, 411-423
8. Straimer, J., Gnadig, N. F., Witkowski, B., Amaratunga, C., Duru, V., Ramadani, A. P., Dacheux, M., Khim, N., Zhang, L., Lam, S., Gregory, P. D., Urnov, F. D., Mercereau-Puijalon, O., Benoit-Vical, F., Fairhurst, R. M., Menard, D., and Fidock, D. A. (2015) Drug resistance. K13-propeller mutations confer artemisinin resistance in Plasmodium falciparum clinical isolates. *Science* **347**, 428-431

9. Mok, S., Ashley, E. A., Ferreira, P. E., Zhu, L., Lin, Z., Yeo, T., Chotivanich, K., Imwong, M., Pukrittayakamee, S., Dhorda, M., Nguon, C., Lim, P., Amaratunga, C., Suon, S., Hien, T. T., Htut, Y., Faiz, M. A., Onyamboko, M. A., Mayxay, M., Newton, P. N., Tripura, R., Woodrow, C. J., Miotto, O., Kwiatkowski, D. P., Nosten, F., Day, N. P., Preiser, P. R., White, N. J., Dondorp, A. M., Fairhurst, R. M., and Bozdech, Z. (2015) Drug resistance. Population transcriptomics of human malaria parasites reveals the mechanism of artemisinin resistance. *Science* **347**, 431-435
10. Chantarasriwong, O., Batova, A., Chavasiri, W., and Theodorakis, E. A. (2010) Chemistry and biology of the caged Garcinia xanthones. *Chemistry* **16**, 9944-9962
11. Han, Q. B., and Xu, H. X. (2009) Caged Garcinia xanthones: development since 1937. *Curr Med Chem* **16**, 3775-3796
12. Zou, M. H., Du, L.Q., Zeng, H., Luo, L.F., Zhang, H.Z., Lu, C.Z. (2007) Advances of development and utilization of Garcinia resources. *Chin. J. Tropic. Crops.* **28**, 122-128
13. Gu, H. Y., Wang, X. T., Rao, S. Y., Wang, J., Zhao, J., Ren, F. L., Mu, R., Yang, Y., Qi, Q., Liu, W., Lu, N., Ling, H., You, Q. D., and Guo, Q. L. (2008) Gambogic acid mediates apoptosis as a p53 inducer through down-regulation of mdm2 in wild-type p53-expressing cancer cells. *Molecular cancer therapeutics* **7**, 3298-3305
14. Huang, G. M., Sun, Y., Ge, X., Wan, X., and Li, C. B. (2015) Gambogic acid induces apoptosis and inhibits colorectal tumor growth via mitochondrial pathways. *World J Gastroentero* **21**, 6194-6205
15. Li, C. L., Qi, Q., Lu, N., Dai, Q. S., Li, F. N., Wang, X. T., You, Q. D., and Guo, Q. L. (2012) Gambogic acid promotes apoptosis and resistance to metastatic potential in MDA-MB-231 human breast carcinoma cells. *Biochem Cell Biol* **90**, 718-730
16. Wang, Y. J., Xiang, W., Wang, M., Huang, T., Xiao, X. Y., Wang, L., Tao, D., Dong, L. Y., Zeng, F. Q., and Jiang, G. S. (2014) Methyl jasmonate sensitizes human bladder cancer cells to gambogic acid-induced apoptosis through down-regulation of EZH2 expression by miR-101. *Brit J Pharmacol* **171**, 618-635
17. Yi, T., Yi, Z., Cho, S. G., Luo, J., Pandey, M. K., Aggarwal, B. B., and Liu, M. (2008) Gambogic acid inhibits angiogenesis and prostate tumor growth by suppressing vascular endothelial growth factor receptor 2 signaling. *Cancer research* **68**, 1843-1850
18. Yang, L. J., and Chen, Y. (2013) New targets for the antitumor activity of gambogic acid in hematologic malignancies. *Acta Pharmacol Sin* **34**, 191-198
19. Chi, Y. H. B. L., Zhan, X. K., Yu, H., Xie, G. R., Wang, Z. Z., Xiao, W., Wang, Y. G., Xiong, F. X., Hu, J. F., Yang, L., Cui, C. X., and Wang, J. W. (2013) An open-labeled, randomized, multicenter phase IIa study of gambogic acid injection for advanced malignant tumors. *Chinese Med J-Peking* **126**, 1642-1646
20. Asano, J., Chiba, K., Tada, M., and Yoshii, T. (1996) Cytotoxic xanthones from Garcinia hanburyi. *Phytochemistry* **41**, 815-820
21. Thoison, O., Fahy, J., Dumontet, V., Chiaroni, A., Riche, C., Tri, M. V., and Sevenet, T. (2000) Cytotoxic prenylxanthones from Garcinia bracteata. *J Nat Prod* **63**, 441-446
22. Wu, X., Cao, S., Goh, S., Hsu, A., and Tan, B. K. (2002) Mitochondrial destabilisation and caspase-3 activation are involved in the apoptosis of Jurkat cells induced by gaudichaudione A, a cytotoxic xanthone. *Planta Med* **68**, 198-203
23. Xu, Y. J., Yip, S. C., Kosela, S., Fitri, E., Hana, M., Goh, S. H., and Sim, K. Y. (2000) Novel cytotoxic, polyprenylated heptacyclic xanthonoids from Indonesian Garcinia gaudichaudii (Guttiferae). *Org Lett* **2**, 3945-3948

24. Batova, A., Lam, T., Wascholowski, V., Yu, A. L., Giannis, A., and Theodorakis, E. A. (2007) Synthesis and evaluation of caged Garcinia xanthones. *Org Biomol Chem* **5**, 494-500

25. Chantarasriwong, O., Cho, W. C., Batova, A., Chavasiri, W., Moore, C., Rheingold, A. L., and Theodorakis, E. A. (2009) Evaluation of the pharmacophoric motif of the caged Garcinia xanthones. *Org Biomol Chem* **7**, 4886-4894

26. Batova, A., Altomare, D., Chantarasriwong, O., Ohlsen, K. L., Creek, K. E., Lin, Y. C., Messersmith, A., Yu, A. L., Yu, J., and Theodorakis, E. A. (2010) The synthetic caged garcinia xanthone cluvenone induces cell stress and apoptosis and has immune modulatory activity. *Mol Cancer Ther* **9**, 2869-2878

27. Guizzunti, G., Batova, A., Chantarasriwong, O., Dakanali, M., and Theodorakis, E. A. (2012) Subcellular localization and activity of gambogic acid. *Chembiochem* **13**, 1191-1198

28. Guizzunti, G., Theodorakis, E. A., Yu, A. L., Zurzolo, C., and Batova, A. (2012) Cluvenone induces apoptosis via a direct target in mitochondria: a possible mechanism to circumvent chemo-resistance? *Invest New Drugs* **30**, 1841-1848

29. Bai, F., Morcos, F., Sohn, Y. S., Darash-Yahana, M., Rezende, C. O., Lipper, C. H., Paddock, M. L., Song, L., Luo, Y., Holt, S. H., Tamir, S., Theodorakis, E. A., Jennings, P. A., Onuchic, J. N., Mittler, R., and Nechushtai, R. (2015) The Fe-S cluster-containing NEET proteins mitoNEET and NAF-1 as chemotherapeutic targets in breast cancer. *Proc Natl Acad Sci U S A* **112**, 3698-3703

30. Vaidya, A. B., and Mather, M. W. (2009) Mitochondrial evolution and functions in malaria parasites. *Annu Rev Microbiol* **63**, 249-267

31. Mather, M. W., Henry, K. W., and Vaidya, A. B. (2007) Mitochondrial drug targets in apicomplexan parasites. *Curr Drug Targets* **8**, 49-60

32. Wells, T. N., Hooft van Huijsduijnen, R., and Van Voorhis, W. C. (2015) Malaria medicines: a glass half full? *Nat Rev Drug Discov* **14**, 424-442

33. Srivastava, I. K., Rottenberg, H., and Vaidya, A. B. (1997) Atovaquone, a broad spectrum antiparasitic drug, collapses mitochondrial membrane potential in a malarial parasite. *J Biol Chem* **272**, 3961-3966

34. Phillips, M. A., Lotharius, J., Marsh, K., White, J., Dayan, A., White, K. L., Njoroge, J. W., El Mazouni, F., Lao, Y., Kokkonda, S., Tomchick, D. R., Deng, X., Laird, T., Bhatia, S. N., March, S., Ng, C. L., Fidock, D. A., Wittlin, S., Lafuente-Monasterio, M., Benito, F. J., Alonso, L. M., Martinez, M. S., Jimenez-Diaz, M. B., Bazaga, S. F., Angulo-Barturen, I., Haselden, J. N., Louttit, J., Cui, Y., Sridhar, A., Zeeman, A. M., Kocken, C., Sauerwein, R., Dechering, K., Avery, V. M., Duffy, S., Delves, M., Sinden, R., Ruecker, A., Wickham, K. S., Rochford, R., Gahagen, J., Iyer, L., Riccio, E., Mirsalis, J., Bathhurst, I., Rueckle, T., Ding, X., Campo, B., Leroy, D., Rogers, M. J., Rathod, P. K., Burrows, J. N., and Charman, S. A. (2015) A long-duration dihydroorotate dehydrogenase inhibitor (DSM265) for prevention and treatment of malaria. *Sci Transl Med* **7**, 296ra111

35. Painter, H. J., Morrisey, J. M., Mather, M. W., and Vaidya, A. B. (2007) Specific role of mitochondrial electron transport in blood-stage Plasmodium falciparum. *Nature* **446**, 88-91

36. Ke, H., Morrisey, J. M., Ganesan, S. M., Painter, H. J., Mather, M. W., and Vaidya, A. B. (2011) Variation among Plasmodium falciparum strains in their reliance on mitochondrial electron transport chain function. *Eukaryot Cell* **10**, 1053-1061
37. Kutner, S., Breuer, W. V., Ginsburg, H., Aley, S. B., and Cabantchik, Z. I. (1985) Characterization of permeation pathways in the plasma membrane of human erythrocytes infected with early stages of Plasmodium falciparum: association with parasite development. *J Cell Physiol* **125**, 521-527
38. Balabaskaran Nina, P., Morrisey, J. M., Ganesan, S. M., Ke, H., Pershing, A. M., Mather, M. W., and Vaidya, A. B. (2011) ATP synthase complex of Plasmodium falciparum: dimeric assembly in mitochondrial membranes and resistance to genetic disruption. *J Biol Chem* **286**, 41312-41322
39. Shaw, G., Morse, S., Ararat, M., and Graham, F. L. (2002) Preferential transformation of human neuronal cells by human adenoviruses and the origin of HEK 293 cells. *FASEB J* **16**, 869-871
40. Elbel, K. M., Guizzunti, G., Theodoraki, M. A., Xu, J., Batova, A., Dakanali, M., and Theodorakis, E. A. (2013) A-ring oxygenation modulates the chemistry and bioactivity of caged Garcinia xanthones. *Org Biomol Chem* **11**, 3341-3348
41. Theodoraki, M. A., Rezende, C. O., Jr., Chantarasriwong, O., Corben, A. D., Theodorakis, E. A., and Alpaugh, M. L. (2015) Spontaneously-forming spheroids as an in vitro cancer cell model for anticancer drug screening. *Oncotarget* **6**, 21255-21267
42. Tisdale, E. J., Slobodov, I., and Theodorakis, E. A. (2003) Biomimetic total synthesis of forbesione and desoxymorellin utilizing a tandem Claisen/Diels--Alder/Claisen rearrangement. *Org Biomol Chem* **1**, 4418-4422
43. Tisdale, E. J., Slobodov, I., and Theodorakis, E. A. (2004) Unified synthesis of caged Garcinia natural products based on a site-selective Claisen/Diels-Alder/Claisen rearrangement. *Proc Natl Acad Sci U S A* **101**, 12030-12035
44. Guinet, F., Dvorak, J. A., Fujioka, H., Keister, D. B., Muratova, O., Kaslow, D. C., Aikawa, M., Vaidya, A. B., and Wellems, T. E. (1996) A developmental defect in Plasmodium falciparum male gametogenesis. *The Journal of cell biology* **135**, 269-278
45. Alin, M. H., Bjorkman, A., and Ashton, M. (1990) In vitro activity of artemisinin, its derivatives, and pyronaridine against different strains of Plasmodium falciparum. *Trans R Soc Trop Med Hyg* **84**, 635-637
46. Tuteja, R. (2007) Malaria - an overview. *FEBS J* **274**, 4670-4679
47. Francis, S. E., Banerjee, R., and Goldberg, D. E. (1997) Biosynthesis and maturation of the malaria aspartic hemoglobinases plasmepsins I and II. *J Biol Chem* **272**, 14961-14968
48. Klemba, M., Beatty, W., Gluzman, I., and Goldberg, D. E. (2004) Trafficking of plasmepsin II to the food vacuole of the malaria parasite Plasmodium falciparum. *J Cell Biol* **164**, 47-56
49. Tamir, S., Paddock, M. L., Darash-Yahana-Baram, M., Holt, S. H., Sohn, Y. S., Agranat, L., Michaeli, D., Stofleth, J. T., Lipper, C. H., Morcos, F., Cabantchik, I. Z., Onuchic, J. N., Jennings, P. A., Mittler, R., and Nechushtai, R. (2015) Structure-function analysis of NEET proteins uncovers their role as key regulators of iron and ROS homeostasis in health and disease. *Biochim Biophys Acta* **1853**, 1294-1315
50. Rukachaisirikul, V., Phainuphong, P., Sukpondma, Y., Phongpaichit, S., and Taylor, W. C. (2005) Antibacterial caged-tetraprenylated xanthones from the stem bark of Garcinia scortechinii. *Planta Med* **71**, 165-170

51. Reutrakul, V., Anantachoke, N., Pohmakotr, M., Jaipetch, T., Sophasan, S., Yoosook, C., Kasisit, J., Napaswat, C., Santisuk, T., and Tuchinda, P. (2007) Cytotoxic and anti-HIV-1 caged xanthones from the resin and fruits of Garcinia hanburyi. *Planta Med* **73**, 33-40

52. Hoye, A. T., Davoren, J. E., Wipf, P., Fink, M. P., and Kagan, V. E. (2008) Targeting mitochondria. *Acc Chem Res* **41**, 87-97

53. Yousif, L. F., Stewart, K. M., and Kelley, S. O. (2009) Targeting mitochondria with organelle-specific compounds: strategies and applications. *Chembiochem* **10**, 1939-1950

54. Mao, P., Manczak, M., Shirendeb, U. P., and Reddy, P. H. (2013) MitoQ, a mitochondria-targeted antioxidant, delays disease progression and alleviates pathogenesis in an experimental autoimmune encephalomyelitis mouse model of multiple sclerosis. *Biochim Biophys Acta* **1832**, 2322-2331

55. Smith, R. A., and Murphy, M. P. (2010) Animal and human studies with the mitochondria-targeted antioxidant MitoQ. *Ann N Y Acad Sci* **1201**, 96-103

56. Long, T. E., Lu, X., Galizzi, M., Docampo, R., Gut, J., and Rosenthal, P. J. (2012) Phosphonium lipocations as antiparasitic agents. *Bioorg Med Chem Lett* **22**, 2976-2979

57. Lu, X., Altharawi, A., Gut, J., Rosenthal, P. J., and Long, T. E. (2012) 1,4-naphthoquinone cations as antiplasmodial agents: hydroxy-, acyloxy-, and alkoxy-substituted analogues. *ACS Med Chem Lett* **3**, 1029-1033

58. Spangenberg, T., Burrows, J. N., Kowalczyk, P., McDonald, S., Wells, T. N., and Willis, P. (2013) The open access malaria box: a drug discovery catalyst for neglected diseases. *PLoS One* **8**, e62906

59. Guo, Q., Qi, Q., You, Q., Gu, H., Zhao, L., and Wu, Z. (2006) Toxicological studies of gambogic acid and its potential targets in experimental animals. *Basic Clin Pharmacol Toxicol* **99**, 178-184

60. Qi, Q., You, Q., Gu, H., Zhao, L., Liu, W., Lu, N., and Guo, Q. (2008) Studies on the toxicity of gambogic acid in rats. *J Ethnopharmacol* **117**, 433-438

61. Zhao, L., Zhen, C., Wu, Z., Hu, R., Zhou, C., and Guo, Q. (2010) General pharmacological properties, developmental toxicity, and analgesic activity of gambogic acid, a novel natural anticancer agent. *Drug Chem Toxicol* **33**, 88-96

62. Yang, J., Ding, L., Hu, L., Qian, W., Jin, S., Sun, X., Wang, Z., and Xiao, W. (2011) Metabolism of gambogic acid in rats: a rare intestinal metabolic pathway responsible for its final disposition. *Drug Metab Dispos* **39**, 617-626

63. Zheng, Z., Ou, W., Zhang, X., Li, Y., and Li, Y. (2015) UHPLC-MS method for determination of gambogic acid and application to bioavailability, pharmacokinetics, excretion and tissue distribution in rats. *Biomed Chromatogr* **29**, 1581-1588

Figure Legend

Figure 1. Chemical structures of gambogic acid (GBA) and related caged *Garcinia* xanthones (CGXs). Cluvenone (**CLV**) defines the structure of the common CGX motif. Hydroxylation at the C_6 and C_{18} centers of **CLV** produces **MAD28** and **MAD44**, respectively.

Attachment of a triphenylphosphonium salt at these hydroxylated sites produces **CR135** and **CR142**, respectively.

Figure 2. The antimalarial effect of CGX compounds in *P. falciparum* parasites. The antimalarial efficiency of CGXs in Dd2 parasites was measured by the ^{3}H-hypoxanthine incorporation assay (Materials and Methods). The x axis indicates the concentrations of a tested compound, and the y axis indicates the percentage of ^{3}H-hypoxanthine incorporation compared to that in no-drug controls. The assays were set up using triplicate wells for each concentration of each tested compound. The averaged data of five independent experiments are shown (n=5).

Figure 3. Viability *P. falciparum* parasites treated with CGX derivatives. Dd2 parasites were tightly synchronized and treated with compounds at 10x EC_{50} concentrations starting at mid-trophozoite stage. Giemsa smears were made for morphological studies with representative images shown in (A). The red arrows in the panel indicate the specific morphological structures not stained by Giemsa. In (B), the percentage of GNB parasites in control and drug treated cultures (**CR135** and **CR142)** is quantified. In (C), the parasitemia at each time point is plotted, as determined by SYBR Green staining and flow cytometry. For each sample, 1,000,000 events were collected and analyzed. The time-course was repeated three times and error bars in (B) and (C) indicate the standard error of three biological replicates.

Figure 4. The food vacuole integrity of *P. falciparum* parasites treated with CR135 and CR142. Representative IFA images show food vacuole morphology in parasites treated with vehicle, CR135, and CR142, individually. Anti-Plasmepsin II polyclonal antibody (rabbit) was diluted 1:1000 and an AlexaFluor 488 conjugated anti-rabbit secondary antibody was diluted 1:350. MitoTracker Red stains active mitochondria.

Figure 5. The mitochondrial morphologies of *P. falciparum* parasites treated with CGX derivatives. (A) Representative images showing mitochondrial morphology in parasites treated with vehicle or compounds for 8 h. (B) Quantitation of the relative fraction of healthy tubular mitochondria in parasites treated with vehicle or compounds for 8 h. For each treatment, mitochondrial morphology was assessed in 200 parasites. This experiment was repeated three times. Error bars indicate the standard error of three biological replicates.

Figure 6. CGX compounds do not target the mitochondrial electron transport chain of *P. falciparum*. The potency of CGX compounds against the mtETC-independent strain 3D7attB-yDHODH was determined with the ^{3}H-hypoxanthine incorporation assay. Calculated EC_{50}s of compounds [nM] against this strain from three independent experiments: **CR135** (58.0±5.7), **CR142** (61.8±6.4), **MAD28** (383.6±19.5), and **SQ129** (101.3±8.1).

Figure 7. Cytotoxicity of CGX derivatives in HEK293 cells. The cytotoxicity of CGX compounds in human HEK293 cells treated for 24 h was determined by an MTT assay (Materials and Methods). For each concentration of each compound tested, triplicate wells were set up. The y axis (% Growth) indicates the percentage of MTT signal in a drug treated sample compared to that in a no-drug control. The average of three biological replicates is shown. Calculated EC_{50}s are listed in Table 1.

Table 1. EC50 values of CR135, CR142, MAD28 and SQ129 in malaria parasites and human cells.

		CR135	CR142	MAD28	SQ129
Dd2	**[nM]**	10.2±2.9	15.0±4.6	267.5±20.5	106.5±13.1
3D7	**[nM]**	12.3±3.5	18.1±3.7	312.4±23.7	99.5±10.2
HEK293	**[µM]**	1.45±0.35	2.21±0.42	1.83±0.14	9.6±0.45

Antimicrobial Agents and Chemotherapy

788 Calculated EC_{50} values and standard errors resulting from 3-5 independent experiments. Please
789 note that data are shown in nanomolar for *P. falciparum* lines Dd2 and 3D7, but in micromolar
790 for HEK293.
791

Antimicrobial Agents and Chemotherapy

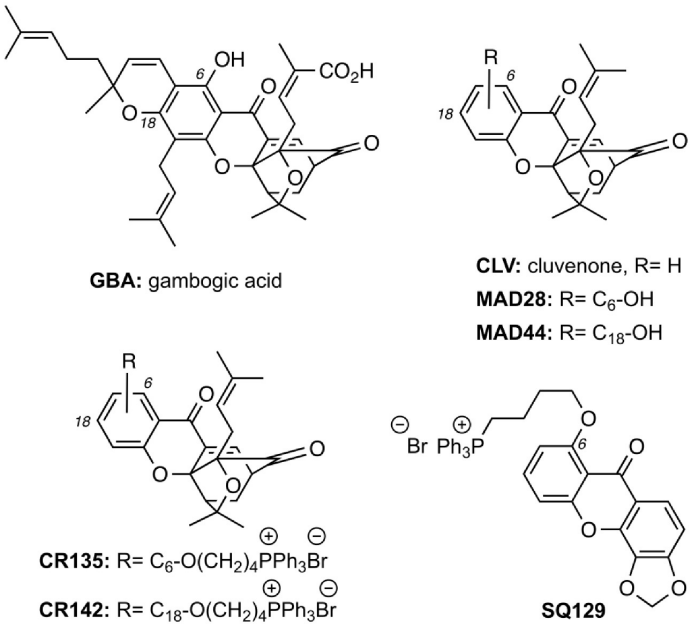

Figure 1. Chemical structures of gambogic acid (GBA) and related caged *Garcinia* xanthones (CGXs).

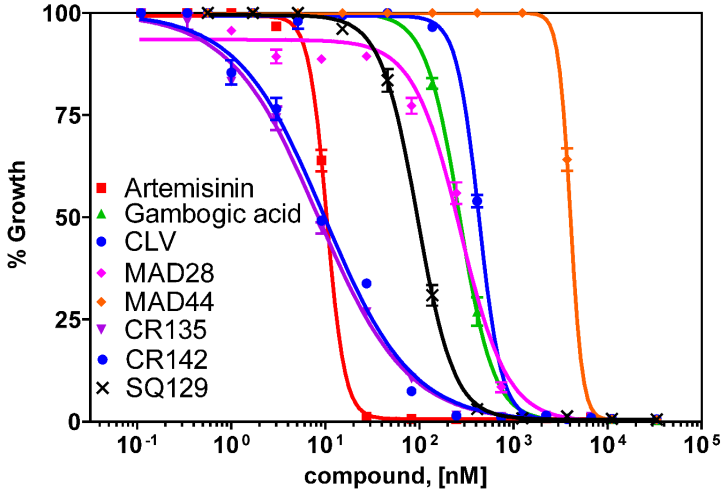

Figure 2. The antimalarial effect of CGX compounds in *P. falciparum* parasites.

Antimicrobial Agents and Chemotherapy

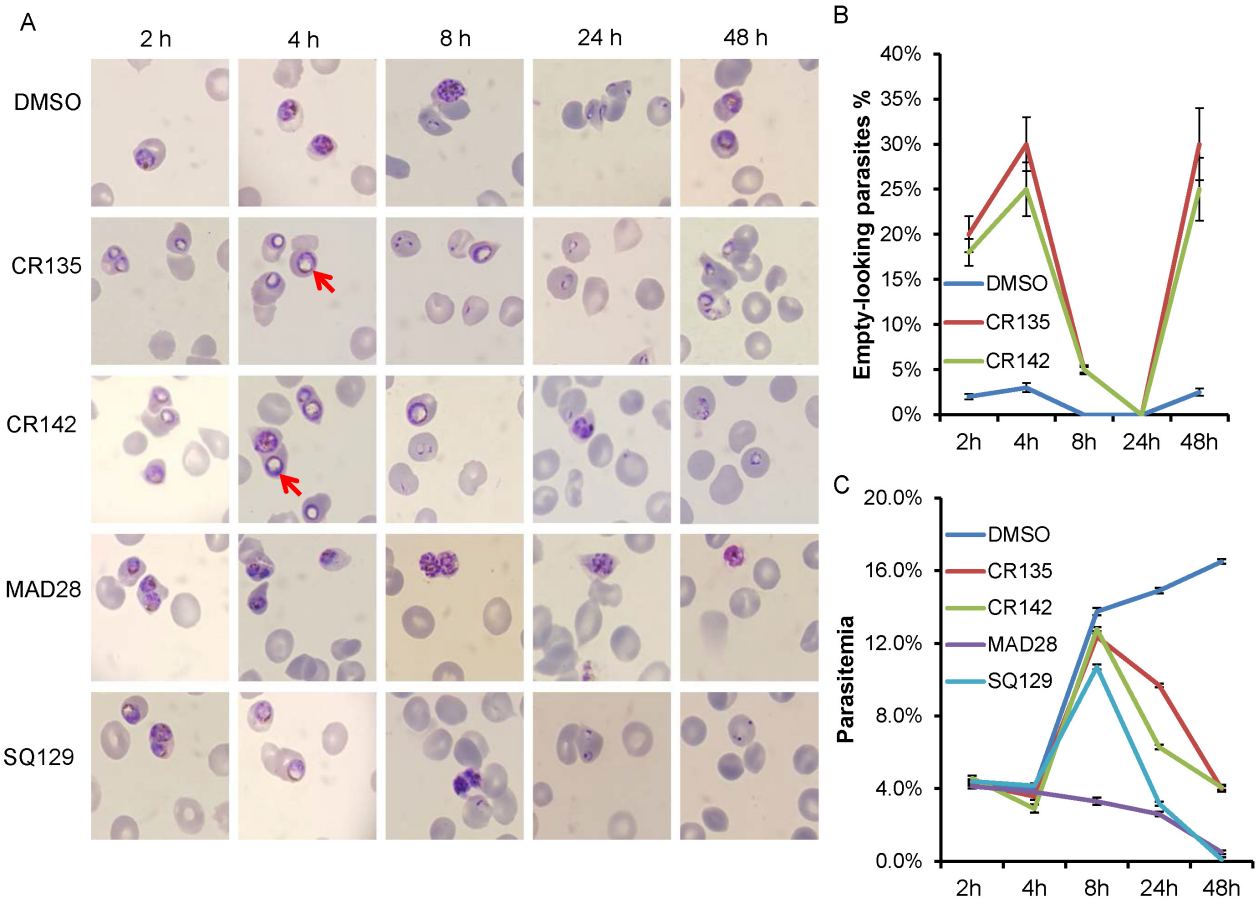

Figure 3. Viability *P. falciparum* parasites treated with CGX derivatives.

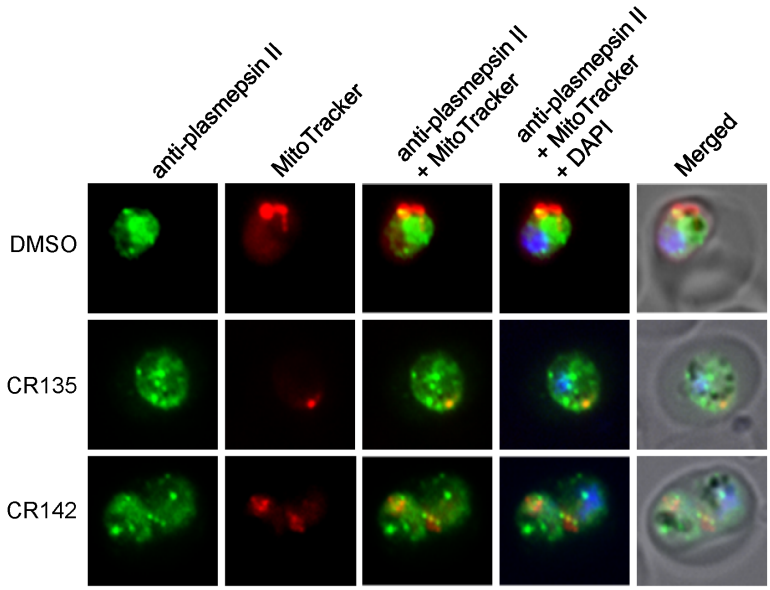

Figure 4. The food vacuole integrity of *P. falciparum* parasites treated with CR135 and CR142.

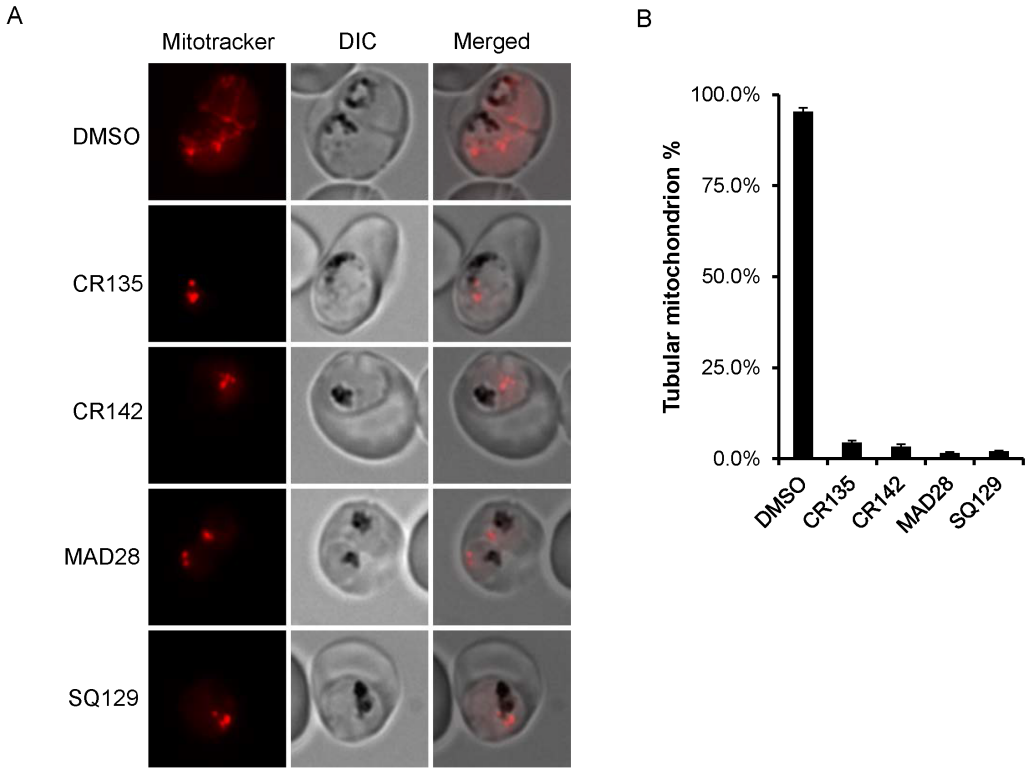

Figure 5. The mitochondrial morphologies of *P. falciparum* parasites treated with CGX derivatives.

Antimicrobial Agents and Chemotherapy

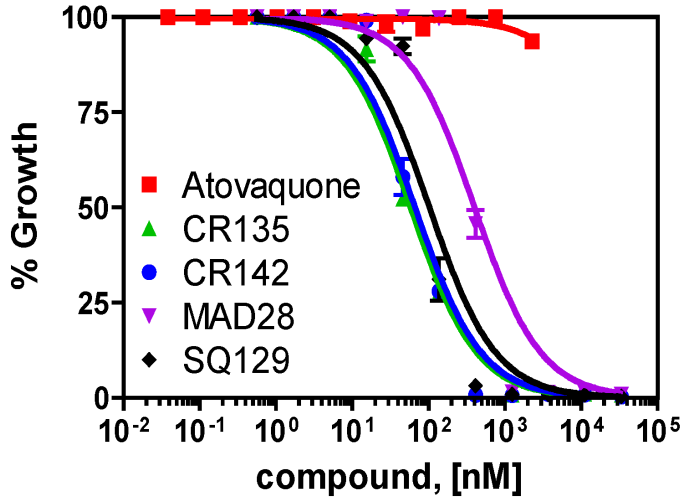

Figure 6. CGX compounds do not target the mitochondrial electron transport chain of *P. falciparum*.

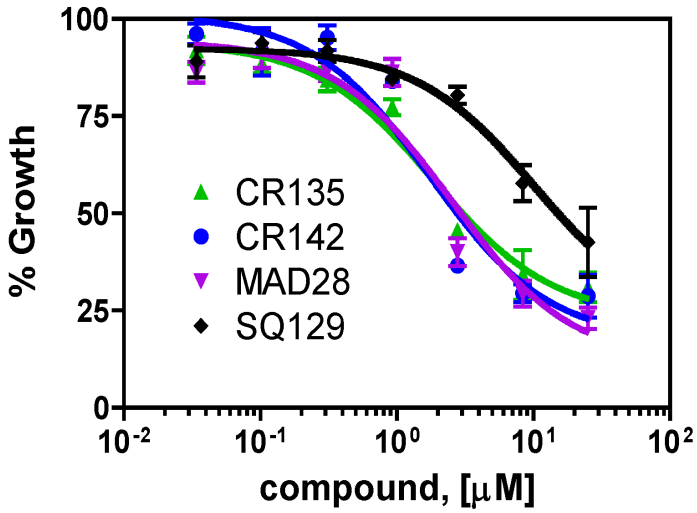

Figure 7. Cytotoxicity of CGX derivatives in HEK293 cells.

Antimicrobial Agents and Chemotherapy